Organisation for Economic Co-operation and Development

ENV/JM/MONO(2020)22

Unclassified English - Or. English

24 September 2020

ENVIRONMENT DIRECTORATE
JOINT MEETING OF THE CHEMICALS COMMITTEE AND THE WORKING PARTY ON CHEMICALS, PESTICIDES AND BIOTECHNOLOGY

CASE STUDY ON THE USE OF INTEGRATED APPROACHES TO TESTING AND ASSESSMENT FOR IDENTIFICATION AND CHARACTERISATION OF PARKINSONIAN HAZARD LIABILITY OF DEGUELIN BY AN AOP-BASED TESTING AND READ ACROSS APPROACH

Series on Testing and Assessment
No. 326

The corresponding annexes are available under the following cotes:
ENV/JM/MONO(2020)22/ANN1.

JT03465711

OECD Environment, Health and Safety Publications

Series on Testing and Assessment

No. 326

CASE STUDY ON THE USE OF INTEGRATED APPROACHES TO TESTING AND ASSESSMENT FOR IDENTIFICATION AND CHARACTERISATION OF PARKINSONIAN HAZARD LIABILITY OF DEGUELIN BY AN AOP-BASED TESTING AND READ ACROSS APPROACH

IOMC INTER-ORGANIZATION PROGRAMME FOR THE SOUND MANAGEMENT OF CHEMICALS

A cooperative agreement among FAO, ILO, UNDP, UNEP, UNIDO, UNITAR, WHO, World Bank and OECD

Environment Directorate

ORGANISATION FOR ECONOMIC CO-OPERATION AND DEVELOPMENT

Paris 2020

About the OECD

The Organisation for Economic Co-operation and Development (OECD) is an intergovernmental organisation in which representatives of 37 industrialised countries in North and South America, Europe and the Asia and Pacific region, as well as the European Commission, meet to co-ordinate and harmonise policies, discuss issues of mutual concern, and work together to respond to international problems. Most of the OECD's work is carried out by more than 200 specialised committees and working groups composed of member country delegates. Observers from several countries with special status at the OECD, and from interested international organisations, attend many of the OECD's workshops and other meetings. Committees and working groups are served by the OECD Secretariat, located in Paris, France, which is organised into directorates and divisions.

The Environment, Health and Safety Division publishes free-of-charge documents in twelve different series: **Testing and Assessment; Good Laboratory Practice and Compliance Monitoring; Pesticides; Biocides; Risk Management; Harmonisation of Regulatory Oversight in Biotechnology; Safety of Novel Foods and Feeds; Chemical Accidents; Pollutant Release and Transfer Registers; Emission Scenario Documents; Safety of Manufactured Nanomaterials;** and **Adverse Outcome Pathways**. More information about the Environment, Health and Safety Programme and EHS publications is available on the OECD's World Wide Web site (www.oecd.org/chemicalsafety/).

This publication was developed in the IOMC context. The contents do not necessarily reflect the views or stated policies of individual IOMC Participating Organisations.

The Inter-Organisation Programme for the Sound Management of Chemicals (IOMC) was established in 1995 following recommendations made by the 1992 UN Conference on Environment and Development to strengthen co-operation and increase international co-ordination in the field of chemical safety. The Participating Organisations are FAO, ILO, UNDP, UNEP, UNIDO, UNITAR, WHO, World Bank and OECD. The purpose of the IOMC is to promote co-ordination of the policies and activities pursued by the Participating Organisations, jointly or separately, to achieve the sound management of chemicals in relation to human health and the environment.

This publication is available electronically, at no charge.

Also published in the Series on testing and Assessment link

For this and many other Environment,
Health and Safety publications, consult the OECD's
World Wide Web site www.oecd.org/chemicalsafety/

or contact:

OECD Environment Directorate,
Environment, Health and Safety Division
2, rue André-Pascal
75775 Paris cedex 16
France
Fax : (33-1) 44 30 61 80
E-mail : ehscont@oecd.org

Forward

OECD member countries have been making efforts to expand the use of alternative methods in assessing chemicals. The OECD has been developing guidance documents and tools for the use of alternative methods such as (Q)SAR, chemical categories and Adverse Outcome Pathways (AOPs) as a part of Integrated Approaches for Testing and Assessment (IATA). There is a need for the investigation of the practical applicability of these methods/tools for different aspects of regulatory decision-making, and to build upon case studies and assessment experience across jurisdictions.

The objective of the IATA Case Studies Project is to increase experience with the use of IATA by developing case studies, which constitute examples of predictions that are fit for regulatory use. The aim is to create common understanding of using novel methodologies and the generation of considerations/guidance stemming from these case studies.

This case study was developed by the EU ToxRisk project team (BIAC) for illustrating practical use of IATA and submitted to the 2019 review cycle of the IATA Case Studies Project. This case study was reviewed by the project team. The document was endorsed at the 4th meeting of the Working Party on Hazard Assessment in June 2020.

The following case study was also reviewed in the project in 2019:

1. CASE STUDY ON USE OF AN INTEGRATED APPROACH TO TESTING AND ASSESSMENT (IATA) AND NEW APPROACH METHODS TO INFORM A THEORETICAL READ-ACROSS FOR DERMAL EXPOSURE TO PROPYLPARABEN FROM COSMETICS, ENV/JM/MONO(2020)16.
2. CASE STUDY ON THE USE OF INTEGRATED APPROACHES FOR TESTING AND ASSESSMENT FOR SYSTEMIC TOXICITY ARISING FROM COSMETIC EXPOSURE TO CAFFEINE, ENV/JM/MONO(2020)17.
3. CASE STUDY ON THE USE OF INTEGRATED APPROACHES FOR TESTING AND ASSESSMENT FOR 90-DAY RAT ORAL REPEATED-DOSE TOXICITY OF CHLOROBENZENE-RELATED CHEMICALS, ENV/JM/MONO(2020)18.
4. CASE STUDY ON THE USE OF INTEGRATED APPROACHES FOR TESTING AND ASSESSMENT TO INFORM READ-ACROSS OF P-ALKYLPHENOLS: REPEATED-DOSE TOXICITY, ENV/JM/MONO(2020)19.
5. CASE STUDY ON THE USE OF INTEGRATED APPROACHES TO TESTING AND ASSESSMENT FOR PREDICTION OF A 90 DAY REPEATED DOSE TOXICITY STUDY (OECD 408) FOR 2-ETHYLBUTYRIC ACID USING A READ-ACROSS APPROACH FROM OTHER BRANCHED CARBOXYLIC ACIDS, ENV/JM/MONO(2020)20.
6. CASE STUDY ON THE USE OF INTEGRATED APPROACHES TO TESTING AND ASSESSMENT FOR READ-ACROSS BASED FILLING OF DEVELOPMENTAL TOXICITY DATA GAP FOR METHYL HEXANOIC ACID, ENV/JM/MONO(2020)21.

7. CASE STUDY ON THE USE OF INTEGRATED APPROACHES TO TESTING AND ASSESSMENT FOR MITOCHONDRIAL COMPLEX-III-MEDIATED NEUROTOXICITY OF AZOXYSTROBIN - READ-ACROSS TO OTHER STROBILURINS, ENV/JM/MONO(2020)23.

These case studies are illustrative examples, and their publication as OECD monographs does not translate into direct acceptance of the methodologies for regulatory purposes across OECD countries. In addition, these cases studies should not be interpreted as official regulatory decisions made by the authoring member countries.

In addition, a considerations document summarising the learnings and lessons of the review experience of the case studies is published with the case studies:

REPORT ON CONSIDERATIONS FROM CASE STUDIES ON INTEGRATED APPROACHES FOR TESTING AND ASSESSMENT (IATA) -Fifth Review Cycle (2019) -, ENV/JM/MONO(2020)24.

This document is published under the responsibility of the Joint Meeting of the Chemicals Committee and Working Party on Chemicals, Pesticides and Biotechnology.

Abstract

There is an anticipated hazard for agrochemicals that inhibit complex I of the mitochondrial respiratory chain to cause toxicity to the nigrostriatal neurons leading to symptoms that reflect Parkinson disease. This effect has been described in an AOP **(Terron *et al.* 2019)** that has recently been accepted and published by the OECD (OECD, 2018). The **aim of this case study was to assess the application of an AOP approach in a read across safety assessment of structurally closely related mitochondrial complex I inhibitors**, deguelin and rotenone (Figure 1).

Epidemiological studies indicate that exposure of workers to rotenone is statistically associated with increased incidence of Parkinson disease (**Dhillon *et al.* 2008; Tanner *et al.* 2011**); moreover, rotenone is used to induce Parkinson phenotypes in experimental animals (**Betarbet *et al.* 2000**). Therefore, rotenone was used as the source substance. Deguelin can induce parkinsonian-like phenotypes in rats (**Caboni *et al.* 2004**). Whether deguelin has such a parkinsonian hazard liability in humans is currently unclear and therefore deguelin was the target substance for this case study.

Based on the AOP we have applied structural modelling approaches to define the binding of rotenone and deguelin to mitochondrial complex I, the molecular initiating event of the AOP. Further, we defined previously established and routinely applied assays that reflect the various key events (KE) in this AOP; some key events that reflect complex multicellular interactions (e.g. inflammation) were not considered. We have integrated multiple human-based *in vitro* test systems to monitor the effects on mitochondrial effects of rotenone and deguelin. Moreover, to assess the effect on neuron toxicity, we have applied high content imaging-based approaches to measure the degeneration of neuronal neurites. Finally, both biokinetic evaluation of cellular exposure to rotenone and deguelin as well as PBPK modelling has been used to evaluate the relevance of the observed effects *in vitro* towards a likely *in vivo* exposure situation.

Results from *in silico* docking to mitochondrial complex I indicate that rotenone and deguelin are structurally highly similar and share a common pharmacophore for the binding. Rotenone and deguelin have similar *in vivo* metabolism profiles and biokinetic behaviour *in vitro* and *in vivo*. Both substances inhibit complex I activity and cause mitochondrial dysfunction, with rotenone being ~3 times more potent than deguelin. Similarly, rotenone is also more potent than deguelin in disrupting neurites. Altogether we conclude that deguelin has a similar mode-of-action as rotenone, but is less potent in its action.

In addition, we conclude that the practical application of an AOP approach through integration of specific technologies and test systems that reflect the AOP molecular initiating event (MIE) and KEs, might find broader application in a read across safety assessment of structurally related substances.

Table of Contents

Tables

Figures

1. Introduction

Deguelin is a naturally occurring compound that has insecticidal activity. It belongs to the class of rotenoids, which are naturally occurring flavonoid compounds that are used as insecticides. Deguelin is a derivative of rotenone, the latter being used as an insecticide and piscicide. The two major rotenoids in the commercial cubé resin pesticide (the root extract from *Lonchocarpus utilis* and *urucu*) are rotenone and deguelin. Since 2008, plant protection products with rotenone cannot be authorised in Europe and piscicide use has only been allowed in Norway (under the biocide regulation).

The primary mode-of-action of rotenone with the biological system is the interfering with the electron transport chain in mitochondria. Rotenone inhibits the transfer of electrons from iron-sulphur centres in complex I to ubiquinone. This affects the creation of usable cellular energy in the form of ATP. Rotenone is the most studied rotenoid and the most abundant rotenoids in cubé resins and strongly inhibits complex I. Rotenone is more potent than deguelin in its pesticidal effect.

Epidemiological studies have shown an association between exposure of workers to rotenone and the occurrence of Parkinson disease (PD) (**Dhillon *et al.* 2008; Tanner *et al.* 2011**). In experimental models, it has been demonstrated that rotenone (**Betarbet *et al.* 2000**) can induce a parkinson-like phenotype through degeneration of the nigrostriatal dopaminergic cells. This is similar to the typical loss of these cells in Parkinson patients. Given the sensitivity of these dopaminergic cells and the application of various complex I inhibitors as plant protection agents, this raises an overall potential hazard by exposure to any complex I inhibitor targeting these dopaminergic cells and causing or enhancing Parkinson-like effects in humans. The rotenoid deguelin can also induce parkinson-like phenotypes in rats (Caboni *et al.* 2004). This raises the possibility that deguelin exposure may lead to PD in humans.

Much research has been performed on the understanding of the mechanism of the degeneration of the nigrostiatal dopaminergic systems in Parkinson's disease. The accumulated knowledge has been critically examined from which a proposed molecular mechanism of dopaminergic neuronal cell injury was derived. This information did culminate in a description of an Adverse Outcome Pathway (AOP) that describes the events how complex I inhibition leads to degeneration and loss of nigrostriatal neurons ultimately leading to parkinsonian motor deficits. This AOP has been published (Terron *et al.* 2019) and recently been accepted by OECD (OECD, 2018; and see Figure 1 for the detailed description of the AOP). The AOP is initiated through the binding by complex I inhibitors tot the NADH-ubiquinone oxidoreductase leading to inhibition of complex I activity (KE1) and subsequent mitochondrial dysfunction (KE2). The mitochondrial dysfunction can trigger impaired proteostasis (KE3) *in vivo* characterised by the accumulation of for example synuclein in the dopaminergic cells which leads to loss of these cells and thereby degeneration of dopaminergic neurons in the nigrostriatal pathway (KE4). The latter can trigger an inflammatory response, which can enhance the further degeneration process (KE5). If this situation advances and many neurons are lost, this would culminate in parkinsonian motor deficits.

Figure 1. Adverse outcome pathway on inhibition of the mitochondrial complex I of nigrostriatal neurons leading to parkinsonian motor deficits.

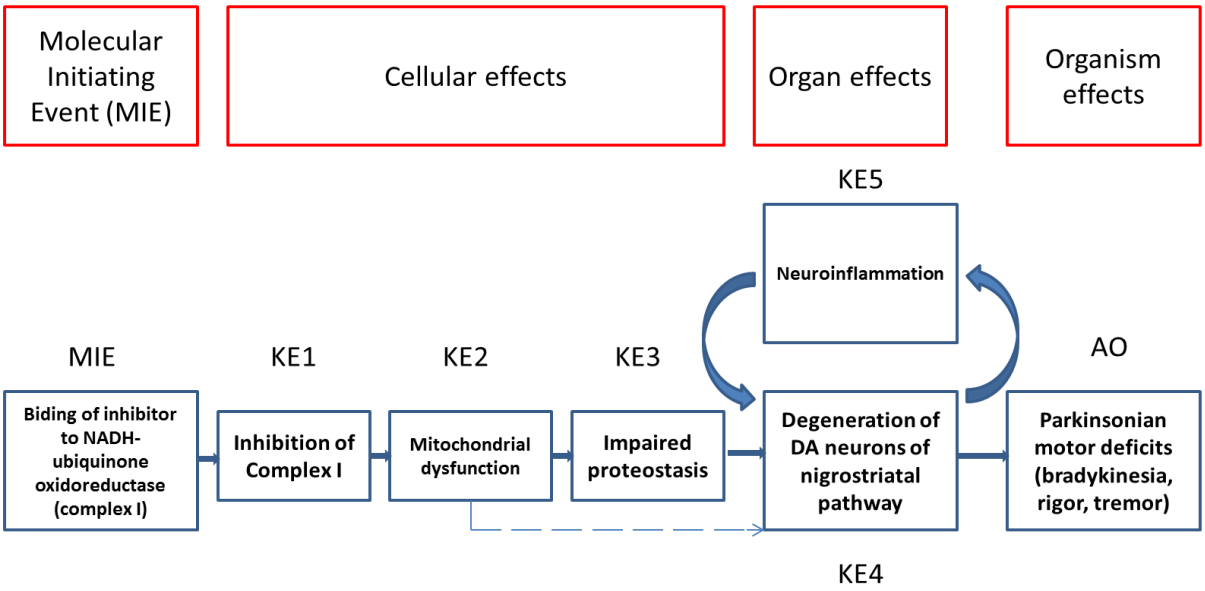

Given the various complex I inhibitors that are currently marketed as plant protection products, exposures to any complex I inhibitor could potentially lead the parkinsonian motor deficits. For the rotenoids, rotenone and deguelin, this effect is described in the scientific literature (**Greenamyre *et al.*, 2001, Caboni *et al.*, 2004**). Repeated exposure of rats to rotenone is often used as a model to study this effect and it is well described in literature, both from *in vitro* and *in vivo* studies (**Betarbet *et al.* 2000**). For other complex I inhibitors less information is known on these potential effects. Preferably testing for such a human hazard should be done without animal experimentation when possible, in particular since the standard *in vivo* repeat dose testing do not investigate the particular part of the brain and furthermore, the motor deficits are only observed when a substantial number of the nigrostriatal dopaminergic cells are lost (**Cheng *et al.*, 2010**). Only when carrying out a repeat-dose neurotoxicity test (TG424) and applying dedicated histopathological analysis the effect can be fully identified and characterised. This is currently not done on a routine basis. Alternatively, to such *in vivo* testing, a battery of relevant *in vitro* tests that represent the various key events of the AOP has been suggested as an approach (**EFSA, 2017**).

The aim of this case study was to uncover whether a battery of tests that represents most of the AOP key events could have an application in the testing of complex I inhibitors for parkinsonian motor deficits. In conjunction with high similarity of rotenone and deguelin, we also considered these two rotenoids as an exemplar set to evaluate whether such an AOP-based testing strategy could be applied in a read across.

2. Purpose

2.1. Purpose of use (targeted regulatory framework)

The purpose of this case study is the **assessment of an AOP-based testing strategy for hazard identification of Parkinson's disease-associated neurological effects caused by chemicals with the goal to provide an IATA test battery for risk assessment of complex I inhibition and liability for parkinsonian motor deficits with a similar MIE interaction as rotenoids.**

The scientific hypothesis is that deguelin would give similar biological interactions and activation of key events as rotenone in the selected test battery that represents the KEs of the AOP but with differences in potency.

The screening strategy is based on the AOP *Inhibition of the mitochondrial complex I of nigrostriatal neurons leads to parkinsonian motor deficits* described on the AOPWIKI (AOP:3). This AOP can be used to support the biological plausibility of this association during the process of evaluation and integration of the epidemiological studies into the risk assessment. It is biologically plausible that a substance triggering the pathway, can be associated with the AO and ultimately with the human health outcome, pending the mode of action (MoA) understanding. In addition, this AOP can be used to support identification of data gaps that should be explored when a chemical substance is affecting the pathway. Moreover, the AOP provides a scaffold for recommendations on the most adequate study design to investigate the *in vivo* apical endpoints. It is important to note that, although the AO is defined in this AOP as parkinsonian motor deficits, degeneration of dopaminergic (DA) neurons is already per se an adverse outcome even in situations where it is not leading to parkinsonian motor deficits, and this should be taken into consideration for the regulatory applications of this AOP. The MIE and KEs identified in this AOP could serve as a basis for assay development that could contribute to an AOP informed-IATA construction, which can be applied for different purposes such as screening and prioritisation of chemicals for further testing, hazard characterisation or even risk assessment when combined with exposure and absorption, distribution, metabolism, and excretion (ADME) information. Given that typically complex I inhibitors are used in plant protection products, this case study falls in the domain of the European Food Safety Authority. We have used rotenoids as a class of complex I inhibitors to evaluate the application of an AOP-based testing strategy.

However, it should be noted that in context of substance evaluation of Registration, Evaluation, Authorization and Restriction of Chemicals (REACH), addressing the risk of the neurodegenerative effect like PD has also recently been requested based on some signals from epidemiological data together with mechanistic data. Further targeted testing has been requested (ECHA, 2018).

So far, the guidelines for hazard assessment of pesticides does not involve new approach methods based on *in silico* and/or *in vitro* methods involving relevant human cell-based test systems. The overall protection goal in the context of our case study is protection against neurological defects in humans. Therefore, in the context of our proposed AOP-based testing strategies there is a requirement to understand the application of different human test systems that could reflect the various KEs of the AOP. This understanding

would define the uncertainty in the application of specific test systems and assays for the use in future screening purposes and also read across approaches based on the AOP.

2.2. Target chemical(s)/category definition

We have selected deguelin as the target chemical. Deguelin is an analogue of rotenone. Deguelin is like rotenone present in cube resins.

Deguelin; CAS 522-17-8

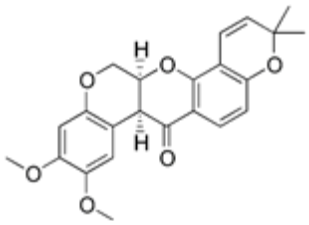

2.3. Endpoint(s) for which the read-across is performed

The health endpoint for which the read-across is performed is Parkinsonian motor deficit disorders caused by complex I inhibitors. This endpoint is not part of standard *in vivo* testing. It may require specifically AOP-based testing strategies. In particular, we have performed a lower Tier testing strategy including both *in silico* approaches as well as *in vitro* assays. These *in vitro* assays have been selected to represent specific key events of AOP describing the complex I inhibition leading to degeneration and loss of nigrostriatal neurons ultimately leading to parkinsonian motor deficits (**Terron *et al.* 2019**; OECD, 2018). Computational structural models have been used to define MIE binding site for rotenone and deguelin. In addition, *in silico* physiological-based pharmacokinetic (PBPK) models have been used to determine human biokinetics of for the rotenoids.

2.4. Exposure information

Not applicable for the read-across case described here.

3. Hypothesis for the analogue approach/category

Deguelin is a potent inhibitor of the respiratory chain complex 1. There is epidemiological evidence that inhibitors of complex I leads to Parkinson's like phenotypes. *In vivo* data indicate that complex 1 inhibitors lead to nigrostriatal neuron degeneration leading to Parkinson's-like phenotypes in rats. Given the potent inhibition of complex I by deguelin, we hypothesise that deguelin has potential liabilities to contribute to Parkinson's disease. There is a datagap on whether deguelin has such a human health hazard.

An AOP has been established and accepted by OECD for complex I inhibition leading to Parkinson's-like nigrostriatal neuron deficits. We have applied this AOP to fill the data gap and have selected various *in silico* and *in vitro* assays that provide insight in the mode-of-action and potency of deguelin on the activation of critical key events as well as on the prediction of human biokinetics of deguelin using PBPK modelling.

3.1. Chemical identity and composition of source chemical

Rotenone is used as the source compound in this case study.

Rotenone; CAS 83-79-4; Purity is 99.9 %

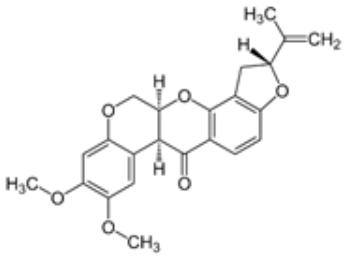

Selection criteria for the selection of the source compound include inhibition of complex I, generation of Parkinson's-like phenotypes *in vivo* and association with Parkinson's health effects in humans. Moreover, the source compound should be highly structurally similar to deguelin.

We have selected rotenone as a source compound. Rotenone is a potent inhibitor complex I of the respiratory chain; it can induce *in vivo* Parkinson's-like phenotype and is associated with Parkinson's disease in epidemiological studies.

We selected rotenone as the source compound, as it is the only structurally similar analogue with these known effects. There are other rotenoid analogues described, but in the context of this case study, we have not been able to work with other structural-related rotenoids since they are neither commercially available nor available at our consortium industry partners. We had to limit ourselves to deguelin and rotenone.

3.2. Physical-chemical properties and other molecular descriptors

Rotenone and deguelin share a common scaffold with a difference of one ring system. The terminal substituted 2-Isopropenyl-2,3-dihydrofuran ring in rotenone is replaced by a 2-Dimethly-2H-pyran in deguelin. Therefore, the two chemicals do possess the same molecular weight, but are slightly different in terms of lipophilicity. See for other molecular descriptors the Table 1, Table 2, Table 3 and Table 4 below; these indicate high similarity

between rotenone and deguelin. Tissue distribution is highly dependent on lipophilicity; and distribution to the brain is critical for the studied health effect in this case study. Several different estimates of lipophilicity of rotenone and deguelin are available from different calculation methods. For rotenone the average predicted log P was 3.83 which agreed reasonably well with the experimental log P value of 4.1. Excluding the low estimate of log P from the Episuite link on the Chemspider website (2.54) an average log P value of 4.26 was obtained. For deguelin no experimental value of Log P was found and the average predicted lipophilicity (Log P) for deguelin was 4.3. The final values of lipophilicity used in the PBPK models were 4.1 for rotenone and 4.3 for deguelin suggesting that deguelin is slightly more lipophilic than rotenone.

Table 1. Compound properties as provided by PubChem

	Rotenone	Deguelin
Property Name	Property value	Property value
Molecular weight	394.423 g/mol	394.423 g/mol
Hydrogen Bond Donor Count	0	0
Hydrogen Bond Acceptor Count	6	6
Rotatable Bond count	3	2
Topoligical Polar Surface Area	63.2A^2	63.2A^2
Monoisotropic Mass	391.142 g/mol	391.142 g/mol
Exact Mass	391.142 g/mol	391.142 g/mol
XlogP3	4.1	3.7
Compound is Canonicalised	true	true
Formal Charge	290	290
Heavy Atom count	3	2
Defined Atom Stereocenter count	0	0
Defined Bond stereocenter count	0	0
Undefined bond stereocenter count	0	0
Isotope atom count	0	0
Covalently-bonded unit count	1	1

Source: https://pubchem.ncbi.nlm.nih.gov

Table 2. LogP values for Rotenone and Deguelin from various sources

Source	Log P	
	Rotenone	Deguelin
Pubchem	4.1	3.7
Toxnet	4.1 (experimental)	
EBI	4.03	4.42
Chemspider	4.65	5.03
Chemspider2	2.54	4.14 (episuite)

Table 3. Water solubility

Source	Water solubility (Mol)	
	Rotenone	Deguelin
EPA*1,2	5.07e-07 (experimental) 8.79e-06 (predicted average)	No experimental data 1.63e-05 (predicted average)

*1: https://comptox.epa.gov/dashboard/dsstoxdb/results?search=Deguelin#properties
*2: https://comptox.epa.gov/dashboard/dsstoxdb/results?search=Rotenone#properties

Table 4. Vapour pressure

Source	Vapour pressure (mmHg)	
	Rotenone	Deguelin
EPA*1,2	No experimental data 1.08e-07 (predicted average)	No experimental data 1.26e-07 (predicted average)
EPA*3	6.9e-10 (at 25 degrees; estimated)	NA

*1: https://comptox.epa.gov/dashboard/dsstoxdb/results?search=Deguelin#properties
*2: https://comptox.epa.gov/dashboard/dsstoxdb/results?search=Rotenone#properties
*3: US EPA; Estimation Program Interface (EPI) Suite. Ver.4.1. Jan, 2011. Available from, as of Sept 1, 2011 http://www.epa.gov/oppt/exposure/pubs/episuite.htm

3.3. Kinetics: Absorption, distribution, metabolism and excretion

There is a limited amount of information on the absorption, distribution, metabolism and excretion of rotenone and deguelin in the scientific literature.

Absorption: The use of rotenone in experimental models of nigrostriatal damage has mainly been following subcutaneous minipump infusion dosing and as such absorption is assumed to be complete by this route of administration.

Distribution: The protein binding of rotenone and deguelin has been determined in human plasma by Cyprotex (CYP1440-R7B). The fraction unbound was reported to be 0.00365 for rotenone and 0.00326 for deguelin at a concentration of 5 µM. Rotenone was also included in the list of ToxCast chemicals whose ADME properties were investigated by Wetmore and colleagues at the Hamner institute; in their hands the measured value of plasma protein binding was 0.017 for rotenone (**Wetmore *et al.*, 2012**).

The protein binding of the two compounds is similar in line with the similar chemical structures and lipophilicity. Using the project developed *in silico* plasma protein binding models the predicted fraction unbound was 0.062 and 0.043 for rotenone using model 1 and model 2 respectively. For deguelin, model 1 and 2 predicted fraction unbound values of 0.054 and 0.063, respectively. The *in silico* estimates of protein binding fraction unbound were about 10-fold higher than the measured values for both compounds. The reason for this discrepancy is unknown but introduces some uncertainty into the values of protein binding that should be used in the PBPK model.

The blood to plasma ratio of rotenone and deguelin was determined in human blood (CYP1440-R7B). The blood to plasma ratio was 0.659 +/- 0.04 for rotenone and 0.671 +/- 0.0195 for deguelin. The compounds show comparable blood cell to plasma partitioning.

The volume of distribution of deguelin following IV dosing was 3.4 L/kg with a large volume of distribution at steady state (30.46 L/kg) due to the triphasic nature of the plasma concentration versus time profile. Using a compartmental model, the half-lives of the three phases were calculated to be 0.09, 1.25 and 9.25 hours.

Tissue levels: Following intravenous dosing to rats (0.25 mg/kg) the tissue distribution of deguelin followed the following rank order heart>kidney>colon>liver>brain>lung. Levels in the perirenal fat increased slowly with time (peaking at 8 hours) and remaining at fairly high concentrations for the duration of the experiment (24 hours) (**Udeani *et al.*, 2001**).

Rotenone and deguelin were dosed subcutaneously to rats using minipumps to give constant drug delivery over the treatment period (**Caboni *et al.*, 2004**). Absorption is assumed to be essentially complete from the sub-cutaneous injection site. At a dose of 3

mg/kg/day for 28 days rotenone caused death (5/23) and punctate loss of tyrosine hydroxylase staining in the nigrostriatal region (2/23), smaller nigrostriatal lesions or reduced tyrosine hydroxylase staining (5/23) and no effect (11/23) in the study group of 23 animals. In a 14 day study at 3 mg/kg/day (n=8), rotenone caused 1 death and 2 nigrostriatal dopaminergic lesions. In 14 days treatment, similar lesions were observed with deguelin at doses of 3 and 6 mg/kg/day. In these studies the brain concentration of rotenone and deguelin were measured.

The rats were arbitrarily assigned into groups based on the measured level of rotenone or deguelin in the brain and the values for the complete dataset are not presented. For rotenone, the brain concentrations showed quite marked inter-individual variability (over a 5-fold range). Deaths were observed in a group of 3 rats where the mean brain exposure was 0.08 +/- 0.03 ppm (=µg/g tissue). There was a trend for more severe lesions in animals with higher brain exposure with 4 out of 5 animals with a reported brain concentration of 0.42 +/- 0.14 ppm exhibiting nigrostriatal lesions or death. The measured concentrations of rotenone in brain and liver of animals dosed with rotenone for 28 days were the same order of magnitude. In the 14 day treatment groups, the liver concentrations were on average about half of those in the brain the reason for this difference is not clear.

No lesions or deaths were observed in animals treated with deguelin at 3 mg/kg/day for 14 days. The brain concentrations in this group were reported as 0.28+/- 0.03 and 0.16 +/- 0.05 ppm (= µg/ml). Toxicity was observed in animals treated with 6 mg/kg deguelin for 14 days the brain levels reported for these animals were 0.24 +/- 0.04 (n=4) and 0.39 +/- 0.08 (N=4) ppm. In most of the animals treated with deguelin the brain concentration was about 3-fold higher than the measured deguelin concentration in the liver.

The levels of 12αβ-hydroxy metabolites were much lower than parent compound levels in the brain for both rotenone and deguelin and no other metabolites were observed in the brain tissue (**Caboni *et al.*, 2004**).

The results in the study by Caboni *et al.* are different from those found by other research groups (**Caboni *et al.*, 2004**). Ravenstijn *et al* (**Ravenstijn *et al.*, 2007**) found no brain lesions after 3 mg/kg/day SC infusion to male Lewis rats but brain lesions were seen after direct intracerebellar injection. In contrast, substantial peripheral toxicity was seen following rotenone infusion. The LD_{50} was determined in mice given rotenone or deguelin by intraperitoneal dosing. The LD_{50} values were 4.3 mg/kg for deguelin and 2.5 mg/kg for rotenone. The brain levels 2 hours after i.p. dosing was 0.39 +/- 0.27 ppm for rotenone and 0.18 +/- 0.09 ppm for deguelin. The liver levels were lower than those in the brain and the only metabolite detected in the brain tissue was the 12αβ-hydroxy metabolite.

Work in this case study suggests that both deguelin and rotenone can interact with efflux transporters that are known to be expressed in the brain. Using *in silico* prediction methods, both compounds were predicted to be inhibitors of breast cancer resistance protein (BCRP) with rotenone also being an inhibitor of P-glycoprotein. This interaction with transporters known to be expressed in the brain is also supported by information in the scientific literature (**Antczak *et al.* 2014; Holvikari and Kidron, 2017; Nt *et al.*, 2005**)[1]. *In vitro* data suggests that rotenone is also a substrate of P-glycoprotein in an ATPase assay (**Lacher *et al.*, 2015**). In this study, the reported Vmax was 16.8 nmol/min/mg protein with a Km of 1.62 +/- 0.51 (µM). This Km concentration corresponds to 0.64 ppm. Although to

[1] https://search.proquest.com/docview/305041769/abstract/9D39ACE322AC4DEFPQ/1?accountid=14682

further confuse the interpretation of data at concentrations up to 100 µM, Lacher saw no inhibition of P-glycoprotein-mediated Rhodamine123 transport.

The effect of P-glycoprotein on rotenone toxicity is controversial. Lacher *et al.* (2015) studied the toxicity of rotenone in LLC-PK1 cells and LLC-PK1 cells transfected with P-glycoprotein. The EC_{50} value for rotenone toxicity increased 2-fold in the presence of P-glycoprotein. However, the effects were not reversed by GF-120918 a potent P-glycoprotein inhibitor. In addition, a second P-glycoprotein inhibitor increased toxicity of rotenone in both the vector transfected and P-glycoprotein transfected cells. This could be explained by the presence of endogenous porcine transporters that have affinity for rotenone and are inhibitable by P-glycoprotein.

In humans, there is limited data available on tissue concentrations of rotenone or deguelin. In a case of a child (3.5 years old) with accidental poisoning exposure to rotenone (estimated dose 40 mg/kg), rotenone concentrations were measured in blood (2.4 ppm), kidney (3.9 ppm) and liver (3.2). In contrast to the data in rats, the brain concentrations were lower than in the liver and below the limit of detection of the assay (< 0.5 ppm) (**De Wilde et al, 1986**).

Dehydro-rotenone is rapidly taken up into the brain with maximum concentrations seen within 15 minutes. Rotenone at a dose of 2 mg/kg/day administered by subcutaneously implantation inhibited dehydrorotenone binding in the brain by 88% (**Talpade *et al.*, 2000**).

Metabolism: The metabolism of rotenone and deguelin by recombinant human CYP isozymes was reported by Caboni *et al* (**Caboni *et al.*, 2004**). Experiments were conducted at a single concentration (~ 36 µM) and the amount of parent and various metabolites at the end of the incubation quantified. For rotenone the ability of the recombinant CYP 2C19 and 3A4 systems to metabolise the compound was similar with 61.9% of parent remaining in the CYP 3A4 incubation and 70.4% remaining in the CYP 2C19 incubation. In the other isozymes investigated more than 87% of parent compound remained at the end of the incubation period. Deguelin was more rapidly metabolised in the recombinant human systems than deguelin with <1% parent observed at the end of the incubation with CYP 2C19 and 33.8% of parent remaining in the incubation with CYP 3A4. CYP 2C19 is known to be polymorphically expressed in the human population with a poor metaboliser phenotype existing in some subjects. For instance in the North-European, Caucasian population 2.4 % of subjects are poor metabolisers for CYP2C19, in Chinese subjects this increases to a frequency of 13% and in Japanese subjects to a frequency of 18%. In subjects with this phenotype, the enzyme activity is zero and the enzyme does not contribute to the metabolism of the compound.

The major metabolites of rotenone and deguelin formed on incubation with human liver microsomes are 12-αβ-hydroxy metabolites in addition both compounds are metabolised by 2-O-demethylation (**Caboni *et al.*, 2004**). The 12αβ-hydroxy metabolites of rotenone and deguelin are less potent inhibitors of complex I compared to the parent compound (**Caboni *et al.*, 2004**).

The metabolic clearance of rotenone was measured in cryopreserved human hepatocytes by Wetmore *et al.* (**Wetmore *et al.*, 2012**) where the intrinsic clearance was measured to be 20.9 and 24.4 ml/min/10^6 cells at a substrate concentration of 1 and 10 µM respectively.

In vivo in the rat the plasma clearance of deguelin was observed to be 4.36 L/h/kg, which equates to a value of 72.7 ml/min/kg. With the assumption that the blood:plasma ratio in the rat is the same as in human 0.671, the blood clearance of rotenone is calculated to be

~100 ml/min/kg, which is equivalent to or slightly higher than liver blood flow in the rat suggesting that first pass metabolism of deguelin would be expected to be high with an extraction across the liver ~1 and a bioavailability close to 0 following oral dosing (**Udeani *et al.*, 2001**). Although no plasma concentrations were reported in the study by Udeani *et al* following oral dosing the dose normalised concentrations in perirenal fat were about 10% of those seen after IV dosing under an assumption that the pharmacokinetics are linear within this dose range..

Excretion: Within 5 days of intragastric administration of [3H]-deguelin 58.1% of the dose was eliminated via the faeces and 14.4% via the urine. Of the administered dose 1.7% was found in the faeces and 0.4% in the urine as unchanged drug suggesting that absorption of the compound is almost complete or that the compound is degraded in the intestinal lumen (**Udeani *et al.*, 2001**).

Table 5. Summary table of ADME for Rotenone and Deguelin

			Rotenone	Deguelin
Absorption	*Subcutaneous minipump infusion dosing*	*in vivo*	Complete absorption assumed	Complete absorption assumed
Distribution	*Binding protein in human plasma CYP1440-R78*	*in vitro*	Unbound from 5µM in 0.00365 bound 0.017	Unbound from 5µM in 0.00326
		in silico	Unbound model 1 = 0.062 Unbound model 2 = 0.043	Unbound model 1 = 0.054 Unbound model 2 = 0.063
	Blood to plasma ratio CYP1440-R78	*in human*	0.659 ± 0.04	0.671 ± 0.0195
			Organ concentrations reported pp (µg/g tissue)	
	Subcutaneously dosing 28 days at 3mg/kg/day	*in vivo*	Brain 0.08 ± 0.03ppm,0.42 ± 0.14ppm	
	Subcutaneously dosing 28 days at 3mg/kg/day	*in vivo*	Brain 0.13 ± 0.00ppm,0.08 ± 0.04ppm	Brain 0.28 ± 0.03ppm,0.16 ± 0.05ppm
	Subcutaneously dosing 28 days at 3mg/kg/day	*in vivo*		Brain 0.39 ± 0.08ppm,0.24 ± 0.04ppm
	Intraperitoneal dosing 3mg/kg/day		Brain after 2h 0.039 ± 0.027ppm	Brain after 2h 0.018 ± 0.09ppm
	Ingestion 3.5 years old, estimate dose 40mg/kg	*in human*	Blood (2.4 ppm), kidney (3.9ppm) and liver (3.2ppm)	
	Intraperitoneal dosing 3mg/kg/day	*in vivo*	LD50 values were 2.5mg/kg	LD50 values were 4.3mg/kg
Metabolism	*metabolites of CYP 2C19*	**functional**	70.5% parent remaining from 36µM	<1% parent remaining from 36µM
	metabolites of CYP 3A4	**functional**	61.9% parent remaining from 36µM	33.8% parent remaining from 36µM
	metabolic clearance	*in vitro*	20.9mL/min/10^6cells at 1µM and 24.4 at 10µM	
	metabolic clearance	*in vivo*	100mL/min/kg	2.7mL/min/kg
Excretion	*5 days intragastic administration*	*n vivo*		60µCi/mL and 2mL/kg 51.8% of dose excreted via faeces 14.4% of dose excreted via urine

3.4. Mode/Mechanism of action or adverse outcome pathways (MOA/AOP); including experimental (NAM) data and *in silico* models – e.g. prediction of MIEs, key events.

Much research has been performed on the understanding of the mechanism of the degeneration of the nigrostiatal dopaminergic systems in Parkinson's disease. The

accumulated knowledge has been critically examined from which a proposed molecular mechanism of dopaminergic neuronal cell injury was derived. This information did culminate in a description of an Adverse Outcome Pathway (AOP) that describes the events how complex I inhibition leads to degeneration and loss of nigrostriatal neurons ultimately leading to parkinsonian motor deficits. This AOP has been published (**Terron *et al.* 2019**) and recently been accepted by OECD (OECD, 2018; and see Figure 1 for the detailed description of the AOP). The AOP is initiated through the binding by complex I inhibitors tot the NADH-ubiquinone oxidoreductase leading to inhibition of complex I activity (KE1) and subsequent mitochondrial dysfunction (KE2). The mitochondrial dysfunction can trigger impaired proteostasis (KE3) *in vivo* characterised by the accumulation of for example synuclein in the dopaminergic cells which leads to loss of these cells and thereby degeneration of dopaminergic neurons in the nigrostriatal pathway (KE4). The latter can trigger an inflammatory response, which can enhance the further degeneration process (KE5). If this situation advances and many neurons are lost, this would culminate in parkinsonian motor deficits.

Figure 2. Adverse outcome pathway on inhibition of the mitochondrial complex I of nigrostriatal neurons leading to parkinsonian motor deficits.

A) Schematic representation of the MIE, KEs and AO belonging to the AOP and their organisation in different types of effects,

B) Table representing all assays discussed in this case study that support the various key events of the AOP.

A)

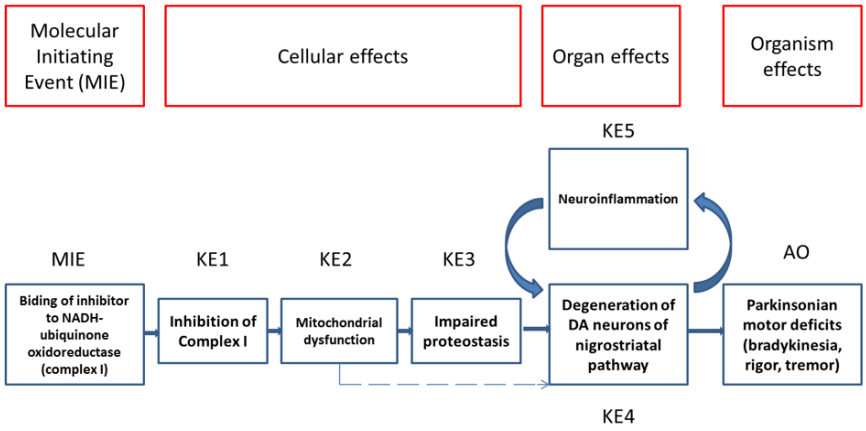

B)

Key event	MIE	KE1	KE2	KE3	KE4	AO
Assay	Receptor Docking studies	Seahorse assay (complex inhibition and whole cell)	Mitochondrial membrane potential assay	Protease activity assay	Viability assays (Resazurin, PI, ATP)	
	Similarity studies			CHOP-GFP expression	Neuronal health (outgrowth and degeneration)	
Key event					**KE5**	
Assay					No assay available	

3.5. Chemical/biological interaction

Here we describe the prior knowledge on the biological targets (e.g. MIE) where rotenone binds. This is essential to provide supportive evidence for the application of the AOP:3 based testing in this case study.

The binding pocket site in complex I is shared by structurally different complex I inhibitors (**Okun, Lu and Brandt, 1999**). Importantly, rotenone-insensitive internal NADH-quinone oxido-reductase of *S. Cerevisae* mitochondria restores the NADH oxidase activity of complex I-deficient mammalian cells and makes these cells insensitive to rotenone. This is indirect supportive evidence indicating that complex I is the direct target of toxicity (**Seo *et al.*, 1998**). Oxidative stress, but not ATP depletion, induces rotenone-induced cell death in SK-N-MC cells. Yet expression of the yeast complex 1 NADH-quinone oxido-reductase, which can take over the role of human NADH oxidase activity, did not display rotenone-induced cytotoxicity, further indicating the role of NADH inhibition. (**Sherer *et al.*, 2003**)

Further studies have indicated the *in vivo* binding sites of rotenone. [3H]-dihydro-rotenone binds to different tissues, with highest accumulation in kidney and heart. NADH enhanced binding occurred the most in the glomerular layer of the olfactory bulb, substantia nigra and some nuclei of thalamus by increasing the number of binding sites, probably by allosteric modulation. (**Higgins and Greenamyre, 1996**). These findings have also suggested possible different isoforms of Complex I that have different sensitivity for NADH-induced modulation.

Binding of rotenoids is not limited to complex I. CheMBL data indicate that rotenone and deguelin share largely similar off-target. Thus, targets in common with active measurements for both deguelin and rotenone: Retineic-acid-receptor-related orphan nuclear receptor (ROR) gamma, CypP450 2C19, p53, U-937. Affinity data is not available for these compounds and also expression and activity of these targets in the SN-DA neurons is not known.

3.6. Responses found in alternative assays (e.g., experimental (NAM) data, *in silico*)

The European Food Safety Authority (EFSA) Scientific Opinion on "Investigation into experimental toxicological properties of plant protection products having a potential link to Parkinson's disease and childhood leukaemia" (EFSA, 2017) and the AOP detail on the data supporting the AOP "Inhibition of the mitochondrial complex I of nigro-striatal neurons leads to parkinsonian motor deficits"[2]. The AOP is based on data with rotenone and MPP+.

In regard to responses found in alternative assays, the following has been identified as a consequence of rotenone treatment and contribute to the weight-of-evidence for the validity of the AOP; suggested are assays that could contribute to AOP-based testing:

KE1: Direct measurement of **inhibition of complex I** has been shown for rotenone in purification of mitochondria from cells where the incubated with NADPH, and an electron acceptor and the flow of electrons is measured. Alternatively, a direct measurement of Complex I activity can be performed. Indirect measurement of complex I is mostly

[2] AOPWiki, AOP: 3 Inhibition of the mitochondrial complex I of nigro-striatal neurons leads to parkinsonian motor deficits; https://aopwiki.org/aops/3

performed on live cells where for example oxygen consumption, intracellular ATP levels, NADH/NAD+ ratios is measured.

KE2: Mitochondrial dysfunction has been measured in isolated mitochondria, intact cells or cells in culture. Mitochondrial dysfunction can be measured by many means such as measuring loss-of function (cellular oxygen consumption, mitochondrial membrane potential, enzymatic activity of the electron transport system and ATP content), gain-of function (mitochondrial permeability transition pore opening, mtDNA damage as biomarker of mitochondrial dysfunction) and generation of ROS and oxidative stress (cellular glutathione, lipid peroxidation, O_2- production, hydrogen peroxide production).

KE3: Impaired proteostasis is measured *in vitro* by an array of different targets such as evaluation of Ubiquitin Proteosomal System (UPS) function (general turnover, proteasome activity, and detection of α-synuclein aggregates), evaluation of Autophagic Lysosomal Pathway (ALP) function (quantification of lysosomes or autophagosomes, monitoring autophagy-related molecules and flux, measuring conversion of the protein LCI-I to LC-II) and evaluation of intracellular transport of e.g. mitochondria and other organelles. SK-N-MC cells have previously been exposed with 5 nM rotenone for up to 4 weeks and proteosomal activity was determined by various methods to observe alpha-synuclein and ubiquitin, DJ-1 distribution, and HEK (human embryonic kidney cells)-GFP (green fluorescent protein) for proteosomal activity (**Betarbet *et al.*, 2006**).

KE4: Degeneration of DA neurons of the nigrostriatal pathway. Progression of neuronal changes with formation of Lewy neurites and reduction of mitochondrial movement leading to cell death has been also observed in-vitro in a chronic cell-based model as well as dopaminergic cell death by inducing LCIII. In postnatal midbrain organotypic slices degeneration of SN-pars compacta neurons after weeks of exposure with 10-50 nM of rotenone occurred. This was indicated by neurite degeneration, morphologic alteration, loss of neurons, decreased TH levels markers for SN-DA neurons and protein oxidation (carbonyl levels). Since this could be blocked by alpha-tocopherol, the neurodegeneration is likely due to damages caused by oxidative stress. (**Testa, Sherer and Greenamyre, 2005**).

KE5: Neuroinflammation. Co-culture experiment with immune cells has shown selective dopaminergic neurodegeneration in neuron/glia cultures.

3.7. Information obtained from other endpoints/species/routes

Acute toxicity *in vivo* data from rotenone and deguelin has also been documented and has followed the usual guideline studies. This allowed observation of general toxicities caused by rotenone and deguelin, but not the more subtle neurodegeneration effects. Deguelin has not be studied in regulatory studies since it has not been marketed itself for pesticide/biocide use. Below we summarise in tables (Table 6, Table 7 and Table 8) the observed data for in particular rotenone.

Rotenone:

The toxicity data on rotenone is summarised below based on the United States Environmental Protection Agency (US-EPA) assessment[3].

[3] Reregistration Eligibility Decision for Rotenone: https://archive.epa.gov/pesticides/reregistration/web/pdf/rotenone_red.pdf

Table 6. Acute toxicity observed upon rotenone exposure

Guideline number	Study Title	MRID	Results	Toxicity
870.1100	Acute oral [rat]	00145496	LD_{50} = 102 mg/kg (M) LD_{50} = 39.5 mg/kg (F)	High acute toxicity
870.1200	Acute dermal [rabbit]	43907501	LD_{50} > 5000 mg/kg	Low acute toxicity
870.1300	Acute inhalation [rat]	42153701	LC_{50} 0.0212 mg/L (combined) LC_{50} =0.0235 mg/L (M) LC_{50} = 0.0194 mg/L (F)	High acute toxicity

Table 7. Repeat-dose toxicity observed upon Rotenone exposure

Rotenone: The toxicity data on rotenone is summarised below based on the US-EPA assessment on the 28th of June 2006.

Guideline number	Study Title	MRID	Results		
			NOAEL (mg/kg/day)	LOAEL (mg/kg/day)	Critical effect(s)
870.3100 82-1b	90-Day oral toxicity (Dog)	00141406 (1980)	0.4	2	BW decreased, inanition
870.3700a 83-3a	Developmental Toxicity (rat)	00144294 (1982)	NA (maternal) 3 (developmental)	0.75 (maternal) 6 (development)	Maternal: Clinical signs (salivation, rubbing of face/paws) Dev: decreased BW
870.3700a 83-3a	Developmental Toxicity (mouse)	00141707 (1981) (main) 00145049 (1981) (range-finding)	15 (maternal) 15 (developmental)	24(maternal) 24(developmental)	Maternal: decreased BW and BW gain Dev: increased resorptions
870.3800 83-4	Reproduction (rat)	00141408 (1983)	0.5/0.6 (parental) 2.4/3.0 (reproductive) 0.5/0.6 (offspring)	2.4/3.0 (parental) 4.8/6.2 (reproductive) 2.4/3.0 (offspring)	Parental(systemic): decreased BW and BW gain Repro: decreased live pups/litters Offspring: decreased BW and BW gain
870.4200	Carcinogenicity (mouse)	40179801a /46274301 (1986)	NA	111/124 (no evidence of carcinogenicity)	Decreased BW
870.4300	Chronic/Oncogenicity (rat)	00156739 (1985) 41657101 (1989 amendment)	0.375	1.88 (no evidence of carcinogenicity)	Decreased BW, BW gain and food consumption

Source: https://myfwp.mt.gov/getRepositoryFile?objectID=50303

They specifically mentioned the risk for neurological toxicity. Furthermore, the results of a literature search identified several studies that proposed a link between developmental neurotoxicity and susceptibility to the chemical in adulthood (Melamed *et al.*, 1990; Eriksson *et al.*, 1993; Eriksson, 1996; Gupta *et al.*, 1999; Thiruchelvam *et al.*, 2002; Barlow *et al.*, 2004).

Table 8. Summary of all proposed or performed neurotox related studies

Guideline number	Study Title	MRID	Results
870.6200a 81-8	Acute neurotoxicity screening battery		Pending results of the subchronic inhalation neurotoxicity study – not available
870.6200 82-7	Subchronic neurotoxicity screening battery		Requested, DCI 2/9/04 (GDCI-071003-20980) -inhalation (rat)
870.6300 83-6	Developmental neurotoxicity		Study required pending results of the subchronic inhalation neurotoxicity study.
	Special studies Subacute neurotoxicity (rat)	45279501 (Betarbet *et al.*, 2000)	Behavioral, biochemical, and neuropathological effects that resemble Parkinson's disease in humans; induction of specific neurodegenerative lesions in nigrostriatal dopaminergic neurons

In vivo (Lewis and Sprague-Dawley rats) studies show that repeated exposure to rotenone (i.v., 2-3 mg/kg/day for 7 days to >5 weeks) generates symptoms that are equivalent to patients with PD. Acute exposure to higher doses generates systemic (cardiovascular) toxicity, non-specific brain lesions. (**Betarbet *et al.*, 2000**). In a study by Caboni *et al.,* rotenone and deguelin were compared for the induction of nigrostriatal dopaminergic system degeneration; the degeneration observed with deguelin was less potent than for rotenone (**Caboni *et al.*, 2004**).

Epidemiological data on the association between pesticide exposure and Parkinson's disease (PD) has been investigated in numerous epidemiological studies which have also been analysed in systematic reviews and meta-analysis (**Ntzani, 2013**). These data have been also been comprehensively discussed in the EFSA opinion of 2017. Overall, a positive and significant association between pesticide exposure and PD was observed. Positive and significant associations for specific pesticides have been found for rotenone.

Deguelin:

Deguelin has not been assessed in terms of pesticide/biocide use and therefore there is no guideline toxicity data published. The compound is being investigated as a potential anti-cancer drug but this is still in the development phase and no safety data has been published so far. The effect of deguelin with respect to neurological effects in rats has been compared to rotenone (**Caboni *et al.* 2004**). Deguelin also causes neurological nigrostriatal dopaminergic system degeneration when administered systemically using mini-pump systems, but is slightly less potent than rotenone, in the order of 2-5, but given the limited dose range, it is difficult to be more precise.

3.8. Information on fate in the environment (hydrolysis, biodegradation)

Not applicable for the read-across case described here.

3.9. The route and duration of expected exposure

Rotenone is used as a pesticide and piscicide and a few epidemiological studies has shown an increase of developing PD with occupational exposure during mixing/loading and application (**Kamel *et al.*, 2007; Dhillon *et al.*, 2008; Tanner *et al.*, 2011**). The main routes of exposure is dermal and inhalation. For these subpopulations a chronic exposure was not considered (i.e. dietary exposure).

4. Source chemicals/Category members

4.1. Identification and selection of source chemicals/category members

Rotenone was selected as the source substance. The basis for this read-across was the AOP on 'Inhibition of mitochondrial complex I inhibition of nigrostriatal neurons leading Parkinsonian motor deficits. There is epidemiological association between rotenone exposure and Parkinson's disease in workers. Moreover, rotenone is often used in experimental animal models to induce Parkinson's-like phenotypes.

Table 9. Chemical name and identity

Compound	Rotenone
Structure	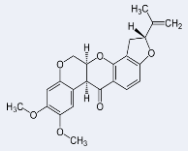
CAS number	CAS 83-79-4
Molecular formula	$C_{23}H_{22}O_6$

5. Data gap filling and Justification

5.1. Data gathering

For our AOP-based testing strategy we have selected a panel of *in silico* and *in vitro* test methods. Below we briefly describe these test systems. More details descriptions for the various test systems can be found in the annex.

5.1.1. MIE: interaction with complex I

We have used structure based modelling (Jain *et al.,* 2017) to evaluate the binding of the target and source compound to complex I. A molecular docking approach was used. Specifically, induced fit docking of Rotenone and Deguelin into Complex I was performed with Schrodinger[4]. The human cryo-EM structure was used (PDB ID : 5XTD). Common scaffold clustering of the resulting docking poses allowed to propose a similar binding mode of the two compounds. This result will be used to build a structure-based pharmacophore model in order to screen large vendor libraries for potential new hits.

5.1.2. KE1: Complex I inhibition.

For measurement of complex I activity we used the Seahorse instrument. This instrument can determine the activity of different mitochondrial respiratory complexes. The activity is based on the oxygen consumption rate using permeabilised cells and the application of specific substrates for complex I. The Seahorse instrument is the gold-standard commercial available instrument that is used in labs worldwide to determine mitochondrial respiratory chain complex activity. The activity of complex I was determined in the neuronal LUHMES cell line that represents dopaminergic neurons.

5.1.3. KE2: Mitochondrial dysfunction

For measuring the mitochondrial dysfunction, we used different assays.

1. Again, the Seahorse instrument was used to determine the oxygen consumption mediated by the respiratory chain. In this case, intact non-permeabilised cells were used in the assay. We used three different test systems: neuronal LUHMES cells, renal RPTEC, and liver hepatoma HepG2 cells; all test systems have functional mitochondria.
2. When complex I of the mitochondrial respiratory chain is blocked the mitochondria cannot establish a mitochondrial membrane potential. Therefore, assessment of the mitochondrial membrane potential is another mean to assess dysfunction of the mitochondria. For this, we have used a high content imaging setup making advantage of fluorescent dyes that accumulate in the mitochondria based on the existence of the membrane potential. The amount of fluorescent dye is dependent on the mitochondrial membrane potential. Using microscopy the levels of the fluorescent dye can be visualised and quantified in individual cells. We have analysed the effect of rotenone and deguelin on the mitochondrial membrane

[4] https://www.schrodinger.com/

potential in two test systems: HepG2 and the neuronal SH-SY5Y dopaminergic neuron cell line.

3. As a consequence of mitochondrial dysfunction, cells cannot produce ATP through the flux of protons through the F0F1ATPase (complex V) of the mitochondria. An indirect measure of mitochondrial dysfunction is therefore the loss of ATP in cells. The ATP levels in cells were determined in HepG2, SH-SY5Y, RPTEC and LUHMES cells.

5.1.4. KE3: Impaired proteostasis

Impaired proteostasis is a complex process. Various cellular perturbations can lead to altered handling of proteins. Two important components are the degradation of proteins through the proteosomal system and the defected processing of proteins after protein translation, where the latter may cause a so-called unfolded protein response in the endoplasmic reticulum. We have used two methods to define the effect of rotenone and deguelin on these cellular functionalities.

1. For the proteosomal activity, we used established fluorescent probe methods. This fluorescent probe is activated by the proteasome. In case that the proteasome is inhibited, limited fluorescence is observed. These experiments have been performed in LUHMES and RPTEC cells.
2. The unfolded protein response results in the activation of one the genes that is induced after ER stress, CHOP. We have used a fluorescent protein reporter that can follow the induction of CHOP based on live cell imaging. This fluorescent GFP-CHOP reporter is induced upon ER stress activation. This reporter is used in the HepG2 hepatoma cell line.

5.1.5. KE4: Degeneration of DA neurons nigrostriatal pathway

For the degeneration of dopaminergic DA neurons we have used assays that report on the phenotypic organisation of DA neurons. This is based on the loss of neurites that can be identified in DA neuron cultures. This assay is based on imaging where cultured neuronal cells are fixed and stained for the actin cytoskeleton, allowing the discrimination of neurites that are extending from the cell body. Image analysis allows the quantification of the neurite outgrowth. Loss of these neurites is representative for degeneration of DA neurons. These assays are performed with LUHMES and SH-SY5Y neuronal test systems.

5.1.6. KE5: Neuroinflammation

For neuroinflammation we do not have an assay included. The neuroinflammation is a process that would also require inflammatory cells in co-culture with our neuronal systems. No data on this KE is integrated in this case study.

5.1.7. In vitro in silico model (bioavailability)

To allow a proper evaluation of the cellular concentrations of rotenone and deguelin, we have used a computational approach to model the intracellular concentrations. The model was validated by measuring the cellular and medium concentration of rotenone using bioanalytical methods. These *in vitro* bioavailability predictions are required for a

quantitative *in vitro* to *in vivo* extrapolation of our *in vitro* data on the KE activation measurements.

5.1.8. PBPK modelling

We used physiology-based pharmacokinetic (PBPK) modelling to predict the *in vivo* brain concentration of rotenone and deguelin. The methodology for PBPK modelling have been based on OECD guidelines. Detailed description of the modelling of rotenone and deguelin can be found in the annex.

5.2. Data and methods

5.2.1. MIE: interaction by Rotenone and Deguelin with the mitochondrial complex I.

For modelling complex I, the human cryo-EM structure has been used (5XTD, **Guo *et al.*, 2017**). Only chains around the, from mutation-studies known, rotenone binding-site (B, C, E, P, N, Q, j and s) have been selected for modelling (**Fendel *et al.*, 2008**). A sequence alignment of the human and the bacterial protein of *Thermus thermophilus and Rhodobacter capsulatus* was done. After performing induced-fit docking of the rotenone and deguelin, the results were clustered according to their common scaffold. (Schrödinger software Maestro2017-4). Subsequently, the RMSD between the two ligands and the protein-ligand interactions have been calculated. From this result, a common binding mode for rotenone and deguelin could be predicted (Figure 3). The chosen pose was used for creating a structure-based pharmacophore model, which further was used for virtual screening (Figure 3). (LigandScout4.2.1)

Figure 3. Docking of rotenone and deguelin in complex I

Left panel: Shared pharmacophore of rotenone and deguelin - Ligand: rotenone; yellow: hydrophobic; red: H-bond acceptor; cylinder: aromatic.

Right panel: Docking poses of rotenone and deguelin into a crystal structure of Complex-I (PDB code: 5XTE): Deguelin-pose: blue, light-grey; Rotenone-pose: pink, dark-grey.

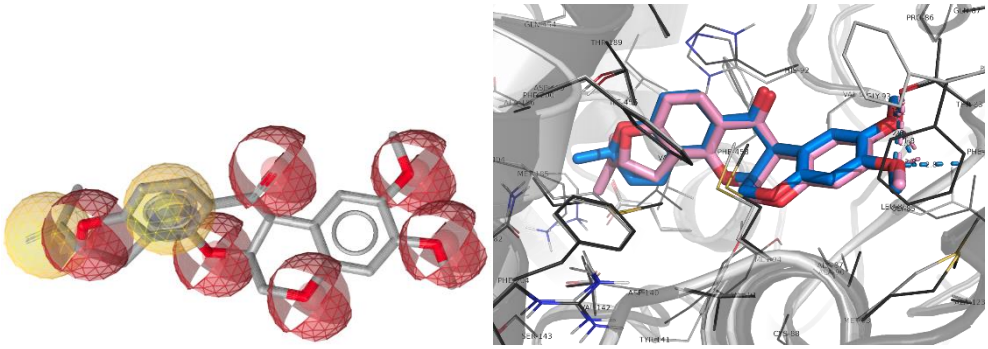

5.2.2. KE1: Complex I inhibition.

The quantification of KE1, inhibition of mitochondrial respiratory chain (MRC) complex I, was performed by permeabilising LUHMES cells and subsequent sequential direct feeding of their mitochondrial respiratory chain (MRC) complexes (Figure 4). For both, the source compound rotenone and the target compound deguelin (10 and 50 µM final concentration, respectively) a strong complex I inhibition (>80% of control) could be

observed, while the other complexes were fully functional. This was also observed for three other complex I inhibitors that served as positive controls (tebufenpyrad 100 µM, fenpyroximate and pyrimidifen 50 µM).

Inhibitors of complex II did not cause an inhibition of complex I, while complex III inhibitors lead to an apparent inhibition of complex I and II activity. This was due to the stall of electrons in the respiratory chain. Since inhibition of complex III and IV can be excluded for rotenone and deguelin, the observed inhibition of complex I is reliable. From the presented experiment, no differences between rotenone and deguelin can be concluded.

Figure 4. Assessment of single mitochondrial respiratory chain complex inhibition.

Proliferating LUHMES cells were plated into Seahorse culture plates and allowed to grow until 90% confluency. Then the cells were permeabilised with digitonin and fed sequentially with substrates for complex I to IV while the respective upstream complex was inhibited. The substance of interest (dissolved in 0.1% DMSO final concentration) was injected prior to the substrates. Inhibition was quantified relative to DMSO control samples.

A) For the source compound rotenone, the target compound deguelin (10 and 50 µM final concentration, respectively) as well as three other complex I inhibitors (tebufenpyrad 100 µM, fenpyroximate and pyrimidifen 50 µM), strong complex I inhibition could be observed, while the other complexes were fully functional.

B) The complex II inhibitor carboxine (100 µM) caused a selective inhibition of complex II, while the other complexes were not affected.

C) The complex III inhibitor antimycin A (50 µM) showed a strong inhibition of complex III as well as impaired activity in complex I and II due to electron stall at complex III.

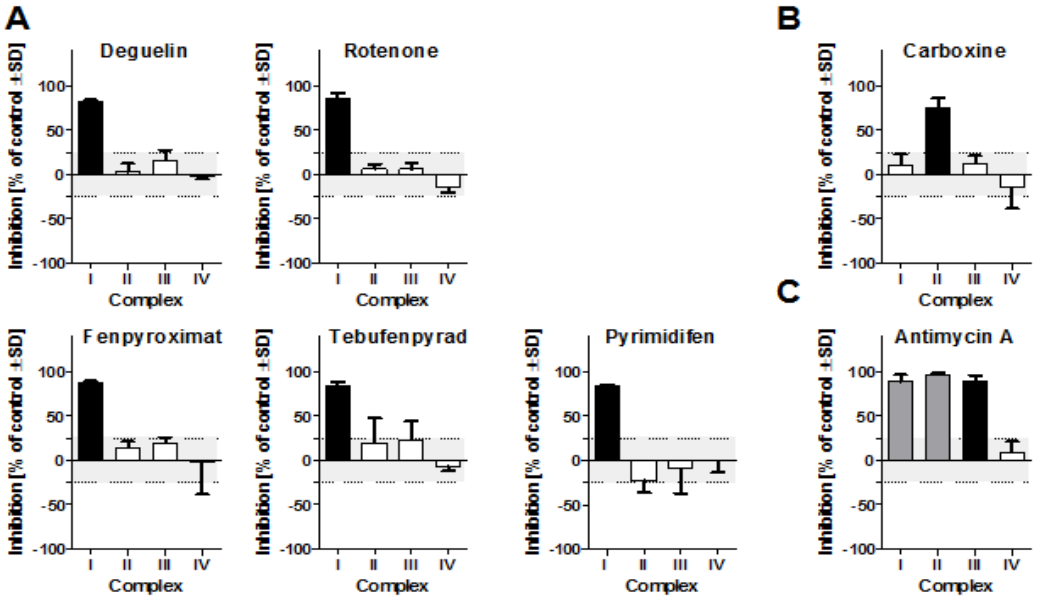

To further assess the potency of complex I inhibition, different concentrations of rotenone and deguelin were investigated for their effect on complex I impairment. Complex I activity was inhibited to 50% by deguelin at concentrations approximately 3 times higher as for rotenone (Figure 5). Thus, it can be concluded that rotenone is 3 times more potent than deguelin.

Figure 5. Assessment of mitochondrial respiratory chain complex I inhibition by rotenone and deguelin.

Proliferating LUHMES cells were plated into Seahorse culture plates and allowed to grow until 90% confluency. Then the cells were permeabilised with digitonin and with substrates for complex I. The substance of interest (dissolved in 0.1% DMSO final concentration) was injected prior to the substrates. Finally, antimycin A and a 10 µM rotenone were injected to determine non-mitochondrial respiration, which was subtracted from the respiration values to yield complex I-mediated respiration. Inhibition was calculated relative to DMSO control samples.

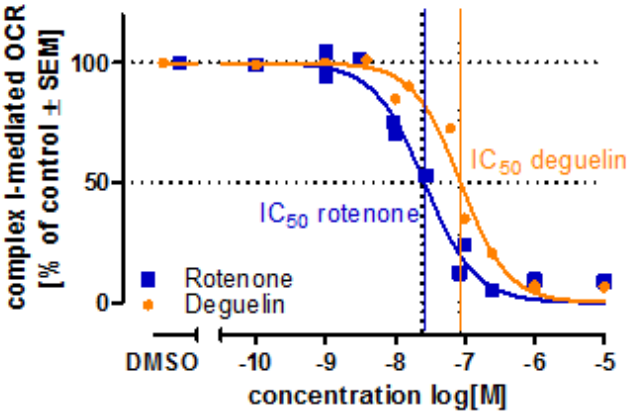

	Rotenone	Deguelin	Potency factor
IC50 perm [nM]	26.4	86.1	3.3

5.2.3. KE2: Mitochondrial dysfunction

i. Effect at oxygen consumption

To investigate the effect of compounds on key parameters of mitochondrial function, oxygen consumption rates (OCRs) were measured directly in whole LUHMES cells using a Seahorse analyser. Basal respiration of whole cells was measured for 20 minutes prior to injection of the test compound, and again after injection for 30 minutes exposure. Changes in OCR upon compound administration give a direct and specific observation of effects of test substance in basal mitochondrial function. An acute injection of rotenone and deguelin (10 µM each) resulted in a complete block of mitochondrial respiration in day 3 LUHMES cells, i.e. the endpoint stage of the neurite outgrowth assay, in which rotenone and deguelin specifically inhibited neurite outgrowth (Figure 6A). No more respiration and free capacities were detectable. Assessment of the compounds' effects in concentration response revealed that rotenone was approximately a factor three more potent than deguelin (IC_{50} ratio deguelin/rotenone) (Figure 6B for LUHMES cells; and Figure 7 for HepG2 cells). Determination of different viability parameters of cells treated for 24 h with increasing concentrations of rotenone (treatment d2-3, as for the neurite outgrowth assay) reveals that basal respiration and respiration linked to ATP production were equally affected while the maximal respiration exhibited a steeper concentration-response curve, however with a comparable IC_{50} value (Figure 6C). Notably, cell viability (assessed by membrane integrity) was not affected at all.

Figure 6. Assessment of mitochondrial dysfunction through quantification of oxygen consumption of intact LUHMES cells on day 3 of differentiation (day of the endpoint quantification of the neurite outgrowth assay).

A) An acute injection of a high, non-cytotoxic concentration (10 µM) of rotenone and deguelin completely inhibits cellular mitochondrial oxygen consumption.

B) Inhibition of total cellular respiration following acute injection of different concentrations of rotenone and deguelin.

C) Effect of rotenone on cells were pre-treated for 24 h before the assay. Concentrations that did not affect general cell viability, did block basal and maximal respiration as well as oxygen consumption linked ATP production completely.

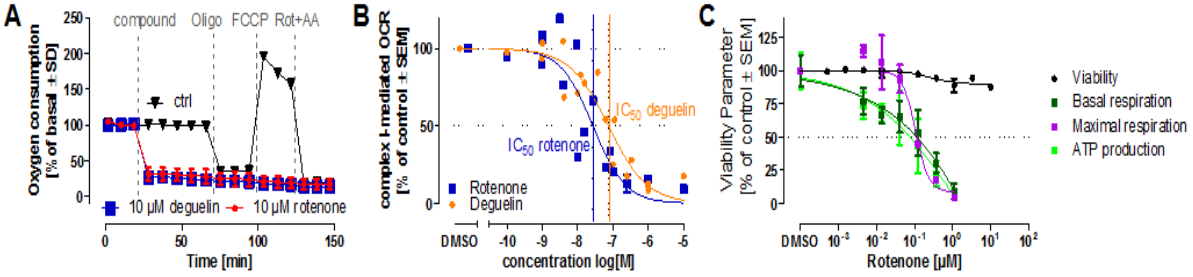

Figure 7. Mitochondrial dysfunction based on oxygen consumption rate measurement in HepG2 cells.

Left) Mitochondrial dysfunction was assessed measuring the oxygen consumption rates and maximal respiratory capacity in intact HepG2 cells. Basal oxygen consumption rates were measured prior to compound injection for 20 min, and after acute injection of toxins for 30 min, effect was normalised to baseline prior to compound injection. Maximal respiration rates are given from OCR upon FCCP injection and normalised to the untreated samples.

Right) BMRs of rotenone and deguelin relative to oxygen consumption rate in HepG2 cells calculated in non-renormalised data sets using the *in vitro* toxicology on-line tool provided by AG. Leist, University of Konstanz.

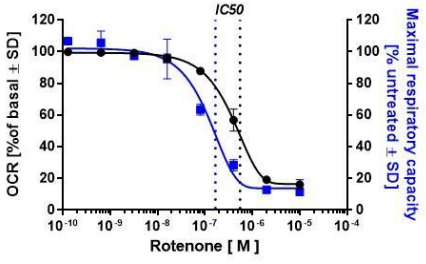

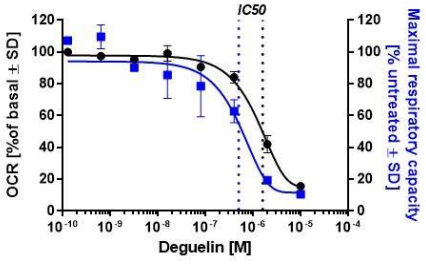

		HepG2 log10 (M)	
		Basal	Max
Rotenone	BMR5	-7.67	-8.18
	BMR10	-7.31	-7.82
	BMR15	-7.09	-7.6
	BMR20	-6.92	-7.44
	BMR25	-6.79	-7.3
	BMR30	-6.66	-7.18
	BMR50	-6.26	-6.78
Deguelin	BMR5	-7.08	-8.05
	BMR10	-6.75	-7.6
	BMR15	-6.55	-7.33
	BMR20	-6.4	-7.12
	BMR25	-6.27	-6.95
	BMR30	-6.16	-6.8
	BMR50	-5.79	-6.3

ii. Effects on mitochondrial membrane potential

To assess the effects on mitochondrial integrity upon chemical exposure, the mitochondrial membrane potential (MMP) was measured using the potential dependent dyes Rhodamine123 or JC-1. Rhodamine123 will diffuse into mitochondria with a potential. A decrease or absence of potential leads to a decrease or absence of dye. In the case of the JC-1 dyes, the presence of a potential leads to accumulation of the dye into the

mitochondria. High concentration of the dye form aggregates and emits light with a wavelength around 561 nm and the not aggregate dye emits light around 488 nm. The data indicate that the both rotenone and deguelin cause a concentration dependent decrease of the MMP. This effect is observed in both SH-SY5Y, HepG2 and RPTEC cells. The potency of rotenone is higher than for deguelin by a factor about three to ten depending on the cell type, indicating that the deguelin and rotenone behave similar in various cell types. The IC_{50} values (BMR50) were also comparable between the three different cell models (Figure 8).

Figure 8. Assessment of mitochondrial dysfunction through quantification of mitochondrial membrane integrity in HepG2, RPTEC and SH-Sy5Y cells.

The membrane integrity was quantified 24h after compound (A; Deguelin or B; Rotenone) exposure based on Rho123 intensity in HepG2 and SH-SY5Y cells and based on JC-1 in RPTEC cells. Curves are an average biological replicates plus standard deviations.

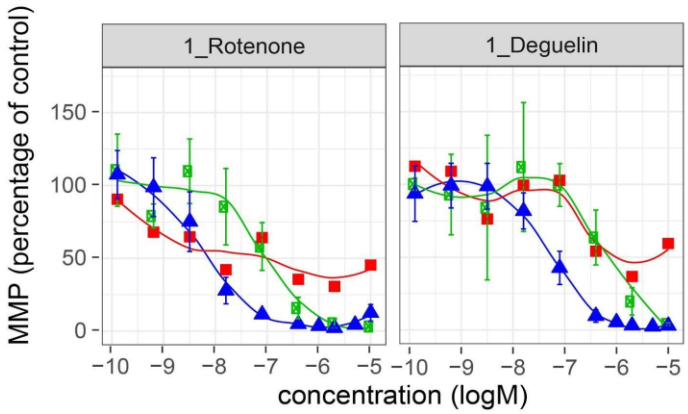

		HepG2	RPTEC	SH-SY5Y
		Log10 (M)		
Deguelin	BMR5	-8,34	-6,56	-7,12
	BMR10	-8,05	-6,53	-6,88
	BMR15	-7,88	-6,51	-6,73
	BMR20	-7,74	-6,49	-6,62
	BMR25	-7,63	-6,48	-6,53
	BMR30	-7,54	-6,46	-6,45
	BMR50	-7,21	-6,35	-6,18
Rotenone	BMR5	-9,15	-10	-8,13
	BMR10	-8,88	-9,75	-7,84
	BMR15	-8,72	-9,57	-7,66
	BMR20	-8,59	-9,42	-7,53
	BMR25	-8,49	-9,29	-7,42
	BMR30	-8,4	-9,16	-7,32
	BMR50	-8,09	-8,4	-6,99

iii. Effect at glycolysis

When cellular ATP production through the oxidative phosphorylation by the mitochondria deplete, then cells may switch to glycolysis to produce ATP. To assess the effect on overall function of the mitochondria, the capacity of the cell to undergo glycolytic switch was addressed based on the production of lactate. Inhibition of the various electron transport chain complexes will perturb the oxidative phosphorylation and force the cell to use glycolysis to deal with energetic demand. The use of the glycolytic pathway leads to the increase of one of the endpoint metabolites lactate. An increase of lactate concentration measured in the supernatant medium indicates an increase in glycolytic rates. We measured the lactate production after exposure to rotenone and deguelin in three different cell types: SH-SY5Y, RPTEC and HepG2 cells (Figure 9). The data indicate that in particular RPTEC and HepG2 cells drastically increase lactate production with increasing concentrations of rotenone and deguelin; this was not observed for SH-SY5Y cells. The effect of deguelin was comparable to rotenone between the cell types, with rotenone having a slightly higher potency in HepG2 cells.

Figure 9. (Left) Assessment of mitochondrial function downregulation by measurement of lactate as indicator of glycolytic switch. Supernatant lactate was measured in RPTEC/TERT1, HepG2 and SH-SY5Y cells after 24 h exposure to a range of concentrations of rotenone and deguelin. Data are represented as percentage of 0.1%DMSO controls and re-normalised to the average of at least two no-effect concentrations (if applicable). (Right) ECs relative to increased lactate production reduction calculated in re-normalised data sets using the point-to-point extrapolation method.

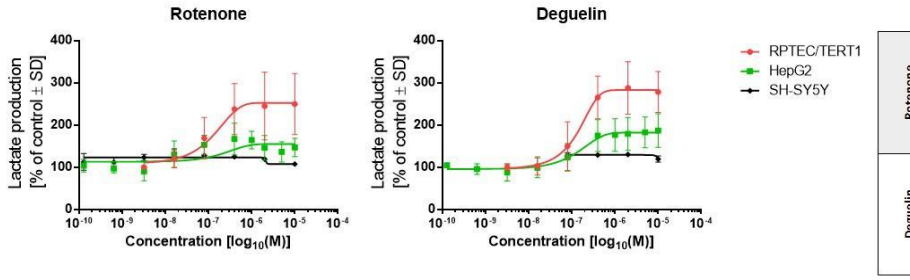

		RPTEC/TERT1	HepG2	SH-SY5Y
		log_{10} (M)		
Rotenone	EC5	-6.8259	-8.37782	NA
	EC10	-6.80	-7.75349	-5.08337
	EC15	-6.78	-7.51	-7.61
	EC20	-6.76	-7.35	-7.14
	EC25	-6.74	-7.24	-6.92
	EC30	-6.72	-7.15	NA
	EC50	-6.65	-6.90	NA
Deguelin	EC5	-6.82	-8.5408	NA
	EC10	-6.80	-7.56	NA
	EC15	-6.77	-7.28	NA
	EC20	-6.75	-7.11	-5.03
	EC25	-6.72	-6.99	-5.24
	EC30	-6.70	-6.90	-5.71
	EC50	-6.62	-6.61	NA

iv. Effect on cell viability

We also investigated the effect of rotenone and deguelin on ATP levels and viability. Since SH-SY5Y neural cells did not compensate the mitochondrial complex I inhibition with a switch to glycolysis, we anticipate that in these cells complex I inhibition would lead to a drop in ATP and a loss of viability as a consequence of reduced cellular ATP levels. ATP was determined used commercial ATP-lite assay. Cell viability was determined by the analysis of the staining of cells with the dye propidium iodide, which cannot enter viable cells, but when cells are dead can pass the membrane and stain the nuclei of necrotic cells. In 3 day, differentiated SH-SY5Y cells both rotenone and deguelin caused a concentration dependent decrease in ATP levels after 120 hr treatment (Figure 10). This was associated with a decrease of cell viability based on decrease of the cells that excluded propidium iodide. Rotenone was more potent than deguelin for both ATP and viability loss.

Figure 10. ATP content and viability measured as propidium iodide exclusion in human neuroblastoma SH-SY5Y cells after exposure to compounds for 24 hrs or 120 h.

The cells were plated at a cell density of 10,000 cells/well and differentiated for 6 days or 3 days prior exposure for 24 h or 120 h, respectively.

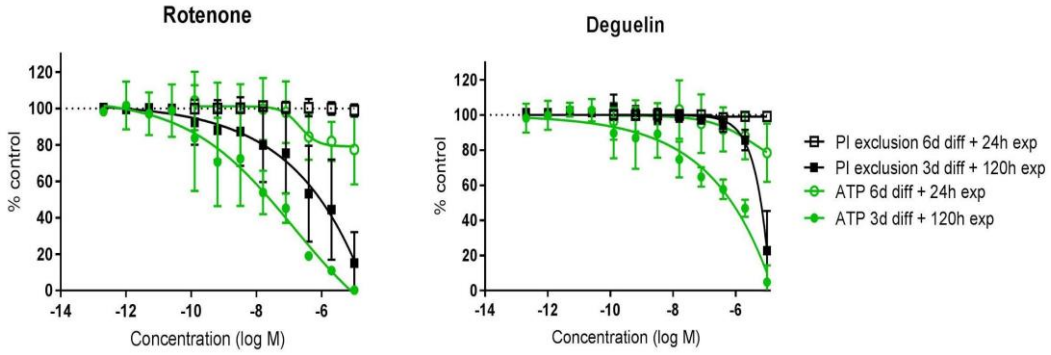

5.2.4. KE3: Impaired proteostasis

Proteosomal activity. To address the question whether the downstream KE3, impaired proteostasis, might be triggered by rotenone and deguelin to a similar extend, proteasomal activity was quantified. Therefore, LUHMES cells, a well-studied and robust representative test system for dopaminergic neuronal cells, were differentiated until day 2 and treated for 24 h with either 10 µM rotenone or deguelin (standard setup of the neurite outgrowth assay). Subsequently, their cell culture medium was replaced by an assay buffer containing a substrate that becomes fluorescent upon proteasomal cleavage. Clearly, both substances inhibited proteasomal activity by >25% at a concentration that does not affect general cell viability (Figure 11). Proteasomal activity was impaired by both, rotenone and deguelin, at concentrations that did not cause cells death (i.e. 10 µM, compare KE4 figures). However, in both treatments, proteasomal activity was impaired at comparable concentrations as ATP was, therefore, an indirect effect of low ATP levels causing decreased proteasome activity, cannot be excluded.

Figure 11. Proteasomal activity of d3 LUHMES cells treated for 24 h with indicated concentrations of rotenone or deguelin.

Cells were exposed for 24 h to the indicated compound, then their medium was exchanged for the assay buffer containing a substrate that becomes fluorescent upon proteasomal cleavage. Rotenone and deguelin inhibited the proteasome by >25% at a concentration that did not affect general cell viability (10 µM).

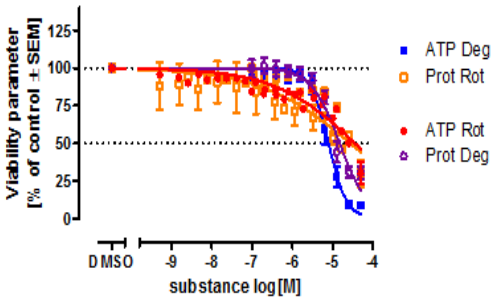

ER stress response. As another measure for disturbances of proteostasis, we evaluated the activation of the unfolded protein response (UPR). Activation of CHOP expression was assessed as an indication for perturbation of the protein translation and folding process. The levels of the UPR related protein CHOP were measured using HepG2 cells stably expressing CHOP-GFP fusion proteins based on the endogenous promoter regions 24h, 48h and 72h after compound exposure. Both rotenone and deguelin induced the expression of CHOP-GFP (Figure 12). The effect was concentration and time dependent with maximal activation observed after 48 hr, well after depletion of the mitochondrial membrane potential. At 48 hr CHOP-GFP induction was observed at ~0.1 µM for rotenone and at ~0.4 µM for deguelin, supporting higher potency of rotenone on this effect. The higher potency of rotenone was also observed for other timepoints. The fact that maximal response was observed at 48 hr, subsequent to mitochondrial perturbations is in line with the AOP concept that the activation of later key events should occur rather subsequent to the onset of earlier key events.

Figure 12. CHOP-GFP expression in HepG2 cells upon 24h, 48h or 72h rotenone or deguelin in a dose range from 0.128 nM up to 10 uM

The CHOP-GFP expression is presented as the fraction GFP positive cells. GFP positive cells have a GFP intensity which is 2x higher than the vehicle condition.

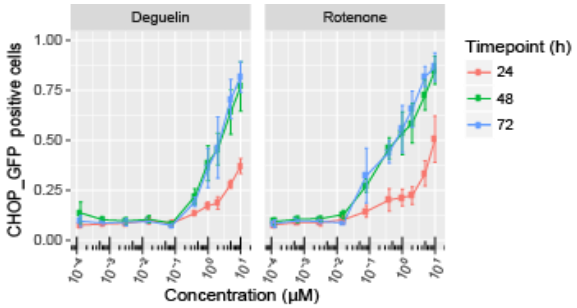

5.2.5. KE4: Degeneration of DA neurons nigrostriatal pathway

i. Neurite outgrowth (LUHMES)

The degeneration of dopaminergic nigrostriatal cells was assessed by the so-called NeuriTox assay. This is a test that was established to identify neurotoxic compounds (**Stiegler *et al.*, 2011; Krug *et al.*, 2013; Delp *et al.*, 2018**). Cells are treated for 24 h during their differentiation and neurite outgrowth for 24 h (day 2-3). Substances that specifically impair neurite outgrowth at concentrations >=4 times lower than they cause general cytotoxicity, are classified as specific neurotoxicants. Both rotenone and deguelin meet these criteria, although rotenone appears to be the more potent compound: the EC_{50} value of rotenone for neurite outgrowth impairment was at 0.3 µM while for deguelin it was at 8 µM - a factor 24 difference (Figure 13).

Figure 13. Assessment of neurite outgrowth inhibition of differentiation LUHMES dopaminergic neurons as established and predictive model for neurotoxicity.

LUHMES cells differentiated for two days were plated at a density of 100,000 cells/cm² (ca. 30,000 cells/well) into 96-well plates, treated one hour later and analysed after 24 h. Complete differentiation (from d0 to d3) was carried out in medium containing either 18 mM glucose or 18 mM galactose. Neurite area (NA) and viability (V, measured by calcein-AM staining) were determined by high content imaging. In parallel, resazurin reduction (Res) and the intracellular ATP content (ATP) were quantified. Concentration-response curves hint to a differential potency of rotenone and deguelin. Both substances did impair neurite outgrowth at concentrations that did not affect general cell viability.

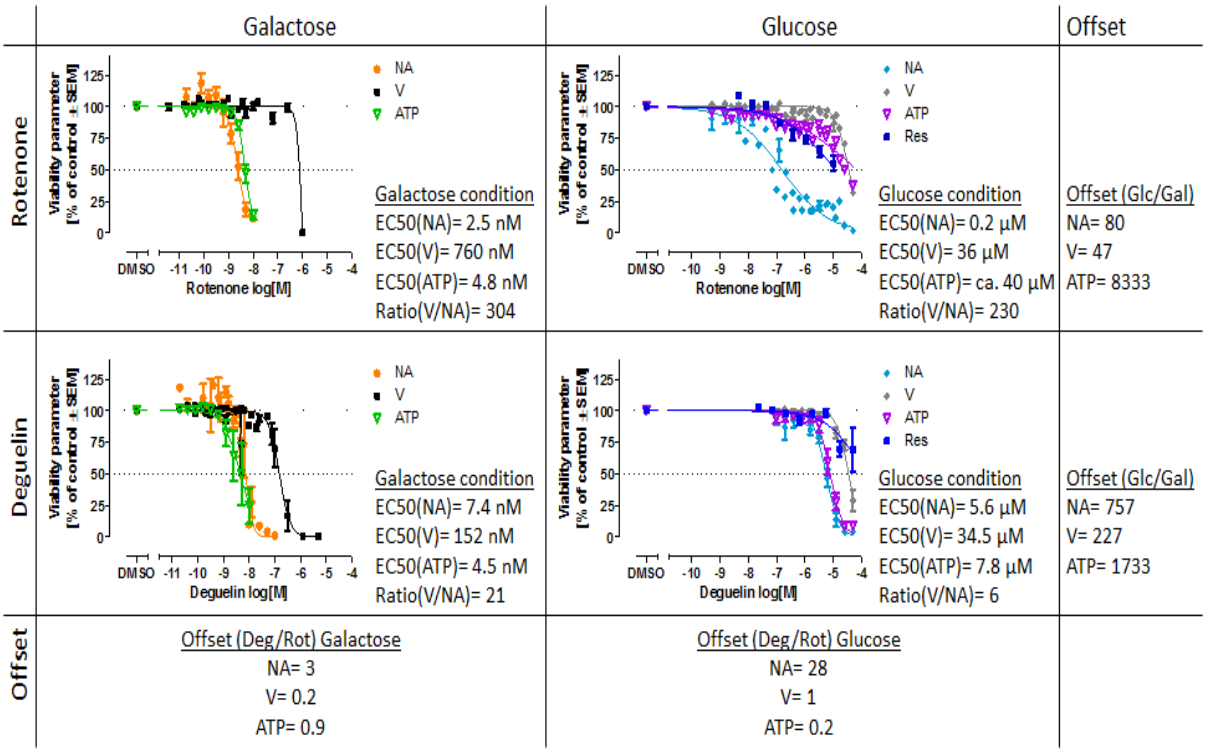

Rotenone and deguelin were tested for their potency to inhibit neurite outgrowth (i.e. the functional endpoint to predict neurotoxicity) in glucose containing medium (=standard established conditions) as well as in galactose containing medium (i.e. experimental condition that makes cells more dependent on mitochondrial metabolism) (Figure 13).

In glucose conditions, general viability parameters, such as membrane integrity (measured by calcein-AM and H-33342 staining) and intracellular ATP content were not strongly different between rotenone and deguelin, thus both compounds can be expected to share their main mode of action. However, neurites were affected at much lower concentrations (ca. factor 30) by rotenone than be deguelin, which is an order of magnitude difference stronger than expected from the mitochondrial function assessment (Figure 13).

Since the glucose conditions allows the cells to compensate for mitochondrial inhibition, the standard assay conditions might not fully assess the hazard of rotenone and deguelin. Therefore, the assay was repeated with galactose as main carbon source instead of glucose. Galactose allows the yield of exactly the same amount of ATP and reduction equivalents as glucose does, but galactose kinetics are much slower. Thus, cells shift from a glycolytic to a mitochondrial phenotype and become dependent on mitochondrial metabolism (Figure 13).

In these galactose conditions, the mean general viability parameters (ATP and calcein-staining) were as well not very strongly different between rotenone and deguelin (Figure 13). Under galactose conditions the offset in neurite susceptibility now yielded a factor 3 three between rotenone and deguelin, compared to a factor >20 under glucose conditions. This is in line with differences in potency between rotenone and deguelin on the mitochondrial function analysis as described for KE1 and KE2. As the galactose conditions do not allow metabolic compensation of mitochondrial inhibition, the difference in neurite susceptibility between rotenone and deguelin resembles the difference assessed for mitochondrial function itself.

ii. Neurite integrity in repeated dose toxicity scenario (LUHMES)

As *in vivo*, humans might not only be exposed to the toxicant once, but repeatedly, this scenario was modelled *in vitro*, accordingly. Technically, this was done by initiation of treatment on d5 of differentiation of the LUHMES cells that were cultured under glucose conditions, followed by a half-medium exchange on day 7 and assay on day 10. Thus substances that were not stable *in vitro* or have certain physico-chemical properties that make them adhere stronger to membranes or plastic will be applied at higher doses, while for stable and hydrophilic substances, no difference should be introduced by the medium change and repeated dosing. As already seen in previous data, rotenone and deguelin exhibit similar responses, however, deguelin displayed to be again less potent. While the EC_{50} for neurite outgrowth for rotenone is at ca. 0.1 µM, it is at ca. 1 µM for deguelin, thus a factor 10 offset (Figure 14).

Figure 14. Assessment of neurite integrity of LUHMES dopaminergic neurons.

Cells differentiated for two days were plated at a density of 150,000 cells/cm² (ca. 45,000 cells/well) into 96-well plates, treated on day 5 and day 7 and analysed at day 10. Neurite area (NA, orange) and viability (V, black) were determined by high content imaging.

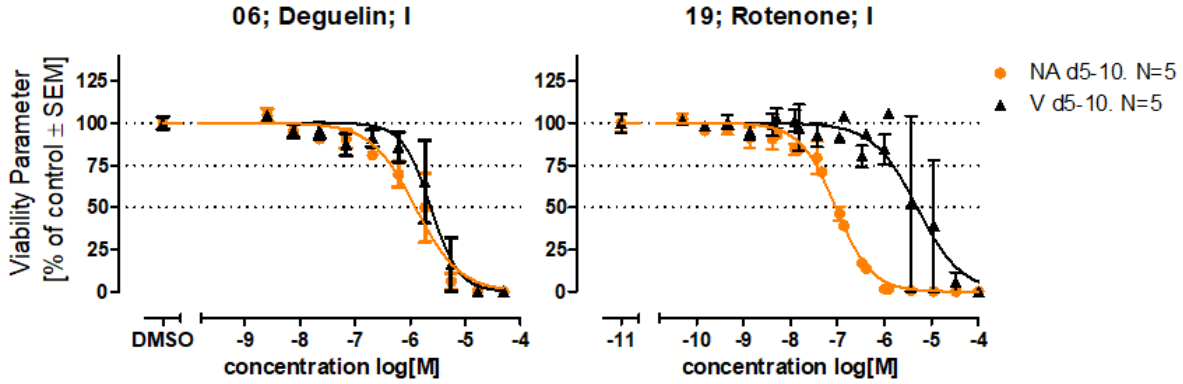

iii. Neurite degeneration (SH-SY5Y)

To assess degeneration of dopaminergic neurons, the change in neurite length after exposure was evaluated in differentiated SH-SY5Y cells. The cells were differentiated for 6 or 3 days and treated with the selected chemicals for 24 or 120 hours respectively. Successively, calcein-AM was used for staining the cytoplasm permitting the measurement of neurite length. Simultaneously, cytotoxicity was measured by propidium iodide exclusion after 24 or 120 hours of exposure. The results are expressed as the percentage of viable cells/mean neurite length in comparison to the DMSO controls. Rotenone caused a

decrease in neurite length while with EC_{50} of around 0.2 µM; in contrast deguelin was less potent and caused a decrease of neurite outgrowth at concentrations >10 µM (Figure 15).

Figure 15. Neurite degeneration measured as mean neurite length and viability measures as propidium iodide exclusion in human neuroblastoma SH-SY5Y cells after exposure to compounds for 24 hrs or 120 hrs.

The cells were plated at a cell density of 8,000 cells/well and differentiated for 6 days or 3 days prior exposure for 24 hrs or 120 hrs, respectively.

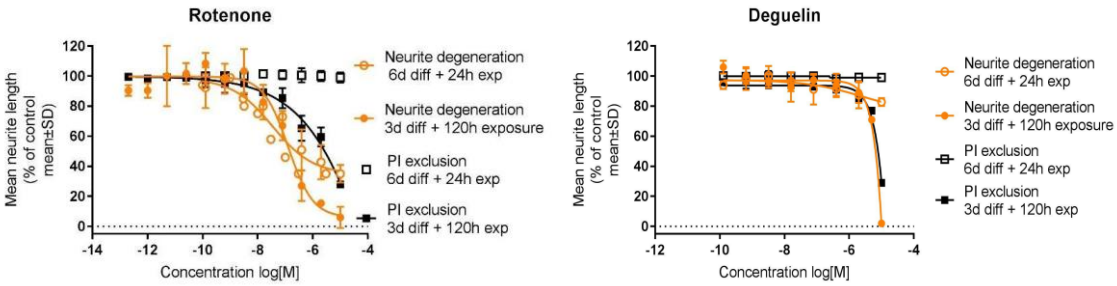

5.2.6. KE5: Neuroinflammation

We have not performed any measured of KE5. Neuroinflammation is a complex process that involves various cell types. There is currently not an *in vitro* assay that integrates various cell types and reliably can assess this key event.

5.2.7. In vitro in silico model

In the test systems we have used nominal medium concentrations to calculate the EC_{50} values for the different assays. Rotenone and deguelin are lipophilic compounds that may result in cellular accumulation of the compounds. This would affect also the overall evaluation of potency of rotenone and deguelin on target inhibition. Therefore we used an *in silico* model to predict the intracellular concentrations of rotenone and deguelin in the different test systems. The *in silico* model takes into account the amount of cells, cell size, incubation volume, culture plates as well as the phys-chem properties of rotenone and deguelin. The predictions indicate a strong accumulation of both rotenone and deguelin in the intracellular compartments (Table 10), with an accumulation factor cell/nominal concentration for the different test systems between ~20 and 375 for rotenone and ~20 and 500 for deguelin (Table 11). No differences was observed in the accumulation factors between rotenone and deguelin. As the compounds are neutral, as expected, the concentrations in the lysosome and mitochondria were predicted to be the same as in the cell.

Table 10. Biokinetic predictions for distribution of rotenone and deguelin in the different EU-ToxRisk *in vitro* assays. The applied nominal concentration was 1^{-6} M (1µM).

Cell Line	Rotenone (M)		Deguelin (M)	
	Media	Cell	Media	Cell
Hep-G2-HULAFE	1.20E-07	3.28E-05	7.67E-08	3.35E-05
Hep-G2-LEIDEN	9.88E-08	2.71E-05	6.31E-08	2.76E-05
LUHMES	6.46E-07	3.75E-04	5.38E-07	4.98E-04
RPTEC	2.88E-07	5.01E-05	2.03E-07	5.64E-05
SHSY5Y	3.18E-07	1.85E-04	2.27E-07	2.10E-04
U2OS	1.79E-07	1.75E-05	1.19E-07	1.92E-05

Table 11. Calculated concentration ratios cell/nominal concentration for different test systems based on the predicted concentrations.

Cell Line	Rotenone	Deguelin
Hep-G2-HULAFE	32.8	33.5
Hep-G2-LEIDEN	27.1	27.6
LUHMES	375.0	498.0
RPTEC	50.1	56.4
SHSY5Y	185.0	210.0
U2OS	17.5	19.2

5.2.8. PBPK modelling

Using the available data the plasma concentrations of rotenone and deguelin were simulated in humans and rats. In humans, the predicted total exposure of either chemical was shown to vary quite widely depending on the value of protein binding used for the simulation. The total exposure to the compound was higher using the measured fraction unbound in human plasma and lower using the *in silico* predicted values of binding in human plasma. These differences lead to some uncertainty in the absolute values of plasma levels that would be expected at a given dose (exposure scenario). Despite this limitation, the extrapolated human exposure data showed that the exposure to the two compounds was comparable when the same method was used to estimate the protein binding of the two compounds (Figure 16).

Figure 16. Median simulated plasma concentrations of rotenone (black solid line) and deguelin (green solid line) following administration of an intravenous 10 mg dose to 100 human subjects (age 20-50; 50% female).

The protein values of 0.00365 and 0.00326 were used for rotenone and deguelin respectively. The 5th and 95th percentiles of the population are shown by dashed lines for rotenone (black) and deguelin (green)

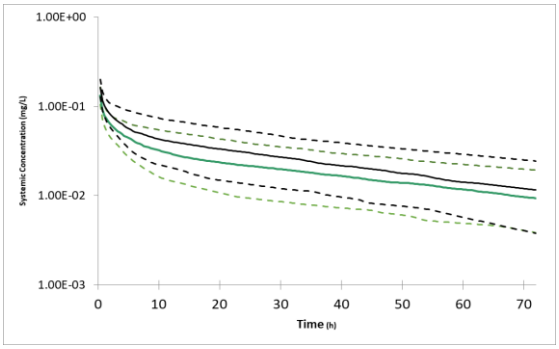

In addition, when the unbound concentrations of the compounds were considered there was similar exposure to both of the compounds when the same dose was administered regardless of the value of protein binding used in the simulations. The protein binding value strongly influences the total concentration of drug in the plasma and tissue but does not have a large effect on the unbound (free) concentration that is mainly dependent on the intrinsic clearance for a low extraction compound (Figure 17). As the free (unbound) concentration of the drug is expected to drive the toxicity, the exposure of the two compounds at the same dose would be expected to be similar within a population of individuals. This supports the use of rotenone as a source compound for the read across to the target compound (deguelin).

Figure 17. Simulated mean plasma exposure to unbound compound after an intravenous dose of 10 mg of deguelin or rotenone to a population of 100 individuals aged 20-50 (50% female).

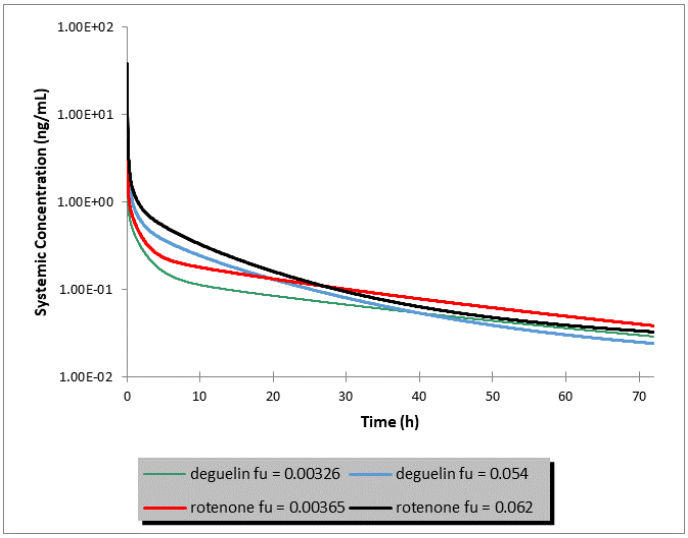

In the rat there were no measured values of plasma protein binding available therefore the fraction unbound values in the rat were estimated assuming that the compounds had the same affinity for albumin in rat and human plasma and that this was the only protein contributing to plasma proteins. Using the observed *in vivo* plasma clearance of deguelin in the rat (2) the volume of distribution of deguelin in the rat was predicted and the predicted value compared with the observed value. Using the estimates of rat plasma protein binding based on the *in silico* model it was possible to predict the Vss and tissue distribution in the brain with a reasonable degree of accuracy.

Likewise when the unbound human clearance predicted from the *in vitro* metabolism data in human hepatocytes was extrapolated to the rat using a single species scaling approach (33) the predicted Cl of deguelin in the rat was closest to the observed values when the *in silico* estimate of rat plasma protein binding was used.

It is difficult to be sure whether this represents a species difference in the protein binding between rat and human or whether there is some limitation with using the measured values of deguelin binding in human plasma. For rotenone where the protein binding was measured in two different laboratories there was ~ 4.5 fold difference in the fraction unbound.

With extrapolated values of clearance and the *in silico* estimate of protein binding the plasma and brain concentrations of rotenone and deguelin were predicted to be similar

when the same dose of compound was administered (Figure 18 and Figure 19). The exposure of the two compounds was predicted to be similar in both the plasma and the brain tissue as were the free plasma concentrations (Figure 18, Figure 19 and Figure 20).

Figure 18. Simulated plasma concentrations of rotenone and deguelin following a 1 mg/kg dose administered as a 24 hour infusion.

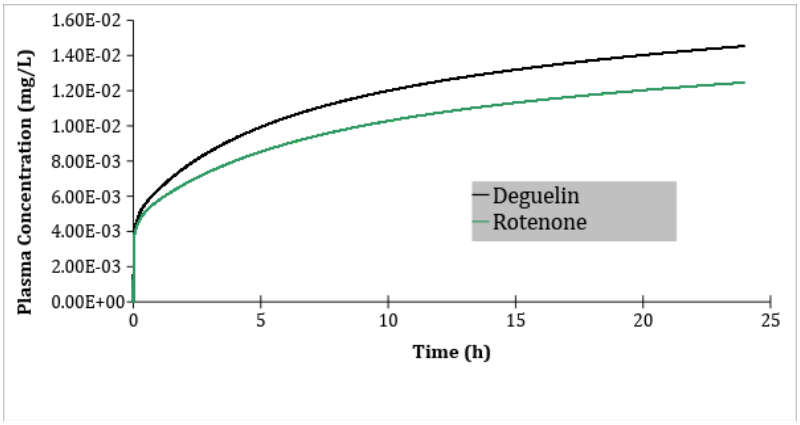

Figure 19. Simulated brain concentrations of rotenone and deguelin following a 1 mg/kg dose administered as a 24 hour infusion.

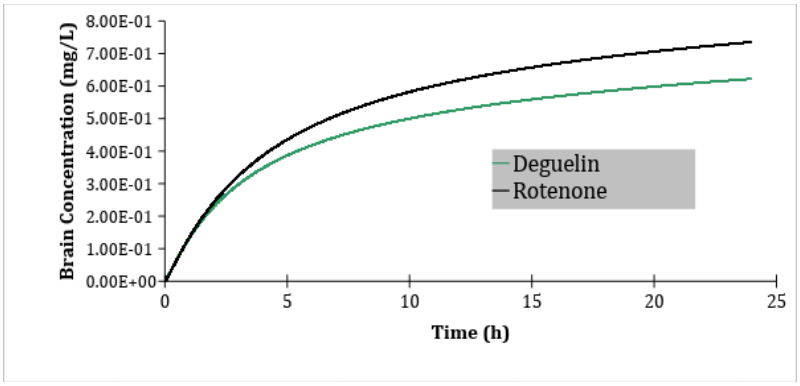

Figure 20. Simulated free plasma concentrations of rotenone and deguelin following a 1 mg/kg dose administered as a 24 hour infusion.

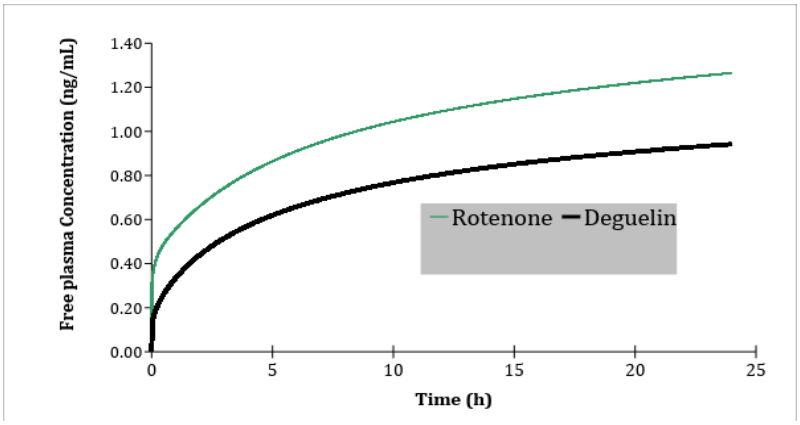

The simulations in paediatric subjects exposed to rotenone were more in line with observed values when the measured value of protein binding was used under these conditions similar concentrations were predicted to occur in blood and liver and kidney and this was in line with the observed concentrations. The use of an *in silico* estimate of plasma protein binding resulted in the predicted concentrations in blood being much higher than the observed values.

The predicted brain concentrations in the paediatric subject were higher than the observed concentration but the reasons for this discrepancy are unclear. Manual sensitivity analysis showed that by adjusting the brain Kp value the concentration in the brain tissue could be reduced to a level that was below the limit of quantification (BLQ) of the analytical method with reasonable predictions of the plasma and tissue concentrations.

Overall, the PBPK modelling data was supportive that under the same dosing level the exposure of an individual to unbound concentrations of deguelin and rotenone would be in a similar range. Simulations in the rat also confirmed that in this species when the predicted model inputs were coming from the same source then the total and unbound concentrations after the same dose of compound were similar.

5.3. Justification

The data support the hypothesis that there is a liability for deguelin to cause Parkinsonian type of effects. This conclusion is based on both a comparison of the physicochemical and biokinetic properties of deguelin and the source compound rotenone, as well as the results from targeted testing involving assays that reflect the key events that lead to the ultimate adverse endpoint. These various data are summarised in the data matrix table (Appendix. Data matrix).

Firstly, the physicochemical properties of deguelin and rotenone are highly similar, both with regard to structural similarity as well as logP value/solubility. Both compounds share the 3D pharmacophore for binding to the complex I. The biokinetics of deguelin and rotenone are highly comparable.

The experimental data also support the common mode-of-action of deguelin and rotenone. This was based on various assays that represent key events for the AOP related to complex I inhibition leading to Parkinsonian nigrostriatal neuronal deficits. Firstly, the mitochondrial oxygen consumption was affected by deguelin and rotenone in different cell types; rotenone was ~3-4 times more potent than deguelin. Secondly, both deguelin and rotenone caused a depletion of mitochondrial function as evidenced by a drop in the mitochondrial membrane potential, with rotenone being ~10-40 times more potent than deguelin. This effect on the mitochondria resulted in an increase in lactate production due to increased glycolysis for both compounds, with deguelin and rotenone being equipotent in two cell types (HepG2 and RPTEC cells) and rotenone being ~40 more potent in neuronal cells. Subsequent assay to address the effect on neuronal degeneration involved demonstrated that deguelin and rotenone both inhibit neurite outgrowth in neuronal cell cultures with rotenone being at least ~3 times more potent. Also, both deguelin and rotenone cause both neurodegeneration with rotenone at least ~10 times more potent.

Based on this integrated testing using *in silico* approaches and the various *in vitro* assays it can be concluded that deguelin shares the same mode-of-action as rotenone, with rotenone being ~3-4 more potent than deguelin.

Taking the AOP key events in consideration, the data are consistent that the various assays contribute to the toxicity of these two compounds.

Since we have only one source compound, we cannot define the inclusion and exclusion criteria for when structural similar compounds would have the same mode-of-action. However, given the consistency of the data between deguelin and rotenone with respect to the various assays that reflect the various tested AOP elements, including the structure-based docking analysis representing the molecular initiation event as well as the various assays representing the key events, an overall high degree of similarity structurally and biologically has been established supporting the case study hypothesis.

6. Strategy for and integrated conclusion of data gap filling

6.1. Uncertainty

Table 12. Uncertainty table

Factor	Uncertainty	Comment
Structural boundary of the read across	Low/medium	The selected source and target chemical belong to the group of rotenoids. They have a common pharmacophore and similar affinity to the mitochondrial complex 1 binding site as determined by structural modelling of rotenone and deguelin I. Yet, we cannot define clear boundaries of the read across, since we only have two chemicals in the read across and lack other positives and negatives. This prohibits to define clear boundaries.
Mode of action/AOP	Low	The rotenoids are pesticides (used as insecticide and piscicide) designed to inhibit the complex I. Epidemiological studies indicate that exposure of workers to rotenone is statistically associated with increased incidence of Parkinson disease; moreover, rotenone is used to induce Parkinson phenotypes in experimental animals. The toxicity potential in humans can be affected by the affinity of the chemicals for mitochondrial complex I. We do not have affinity measurements. We determined that the gene sequence for the various mitochondrial complex I subunits are well preserved between species. Hence, we anticipate a similar mode of action in humans. Our data indeed indicate this: The inhibition of complex I measured based on the mitochondrial respiration in permeabilised neuronal cells demonstrated an efficient blocking of the complex I, without affecting other complexes. This indicates selectivity for blocking complex I of the respiratory chain. Moreover, both rotenone and deguelin potently inhibited overall cellular oxygen consumption and caused rapid depletion of the mitochondrial membrane potential, further supporting the anticipated mode-of-action.
Hypothesis used for the read across for neurotoxicity via mitochondrial complex 1 inhibition	Medium	The hypothesis for the read across is based on a published and OECD accepted AOP. (OECD, 2018). The AOP is based on scientific observations for rotenone. Based on the approved AOP test systems have been selected that represent the activation of the various KE. However, as: • the prediction is based only on *in vitro* and *in silico* assays, and • AO is *in vivo* endpoint (neuron degeneration leading to Parkinson disease), and We propose uncertainty to be "Medium".
Similarity of source chemicals for read-across	Low	The rotenoids (deguelin and rotenone) are similar in their mode of action and demonstrate a high structural similarity. Moreover, using structural modelling we determined the pharmacophore for binding complex I. The pharmacophore covers 4 identical ring structures with only a fifth lactone ring structure being slightly different. In addition, the chemicals have similar physchem and ADME properties.
Phys/Chem	Low	We have retrieved the phys/chem properties for deguelin and rotenone from different sources in the public domain. The results from different sources are highly comparable/identical. This is expected from the highly similar structures between deguelin and rotenone that are common in 4 identical ring structures with only a fifth lactone ring slightly different in structure.
Toxicokinetics	Low	The metabolism of rotenone and deguelin are similar. Moreover, PBPK modelling also demonstrates that the predicted *in vivo* kinetics are similar. Therefore, we anticipate low uncertainty on differences in toxicokinetics between deguelin and rotenone.
Similarity of supportive data	Low	<u>*in vivo*</u> Epidemiological studies indicate that exposure of workers to rotenone is statistically associated with increased incidence of Parkinson disease; moreover, rotenone is used to induce Parkinson phenotypes in experimental animals. While the *in vivo* study setup in the experimental models for rotenone-induced Parkinsonian-like phenotypes is not a guideline study, various different laboratories have applied this method. Importantly, both deguelin and rotenone can induced similar Parkinsonian-like phenotypes (see Caboni *et al.* 2004).
	Medium	<u>*in vitro*</u> Various *in vitro* test system applied are not OECD approved methods. Yet, most of the test methods are well documented (see Annex 1). Moreover, for oxygen consumption measurement we make use of well-established commercial equipment with clear guidelines and protocols for use. All test systems are standardly and routinely used in the various laboratories and applied in various case studies in the context of the EU-ToxRisk project.

		For all *in vitro* experiments we have used DMSO as the solvent. While DMSO itself may have some influence on cells, yet not affecting gene transcriptional responses or any viability measures, we cannot exclude altered cellular uptake of the compounds in this case study. We however assume that the use of DMSO will have limited effect here, since rotenone and deguelin are highly lipophilic and will distribute to the lipophilic cell compartments, including organelles, very effectively.
Quality of end point data	Medium	<u>Uncertainty of the assay</u> The different *in vitro* NAM methods used for addressing our read across case do not have an excepted guideline document. However, they all have a consortium-wide reviewed description document. Various of the assays are described in a DB-ALM document: • Seahorse oxygen consumption = no DB-ALM (uncertainty = low; since company established protocols available) • ATP measurement = no DB-ALM (uncertainty = low, since standard commercial ATP-lite assay kits used) • MMP = created DB-ALM (uncertainty = low, highly reproducible assay available) • Lactate assay = no DB-ALM (uncertainty = low, standard commercial methods available to determine lactate in culture medium) • proteostasis => no DB-ALM (uncertainty = medium, proteostasis is a complex process and the assays used may not represent all the components that represent proteostasis, but methods used are evaluated with positive control in parallel) • neuron outgrowth = DB-ALM (uncertainty = low, well established assays at partner institutes and standard operating procedures available) All methods are only internally validated. However, Various assay types are commonly used to address mitochondrial functioning in *in vitro* systems. The assays are performed in various lab. This can lead to differences in the execution concerning chemical usages, chemical exposures, data analysis, etc. The overall conclusions regarding the effects and potency of rotenone and deguelin are comparable between the different labs and test systems, providing sufficient weight of evidence providing low uncertainty for the overall outcome of the different test systems. Given that most assays did not undergo official validation, we can only rely on the overall robustness of the assays as described under the DB-ALM and the comparison to positive controls used in these assays. The different *in silico* NAM methods regarding the structural modelling are not externally reviewed; since well established structural modelling approaches have been used that are used in the scientific research community we consider the uncertainty low. For the PBPK modelling standard procedures are followed according to OECD guidelines. For the *in vitro* prediction models we have not yet validated the cellular exposures for rotenone and deguelin and cannot validate the differences in cellular uptake. We consider the uncertainty medium.
	Low-Medium	<u>Following proposed AOP</u> This read across for the nigrostriatal dopaminergic neuronal degeneration health effect makes use of a reviewed and accepted OECD AOP. Although high certainty is available on early key events of the AOP, the uncertainty may increase for the role of later key events in the AOP. The literature has defined modes-of-action of deguelin in relation to a pro-claimed anticancer activity. This deguelin anticancer activity is claimed to be related to modulation of specific kinases, e.g. Akt, Aurora kinase, Hsp90 (Baba *et al.* 2015; Lu *et al.* 2017; Oh *et al.* 2007). These mode-of-actions are not part of the AOP. The role of these interactions in the relation to the parkinsonian-related adverse endpoint is fully unclear and not considered at a contributor to the AOP. An involvement cannot be excluded, yet potency for inhibition of these targets is higher than inhibition of complex I. Moreover, these additional effects could be related to secondary responses as a consequence of mitochondrial toxicity.
	Low-Medium	<u>Key events of assays reflected by assays</u> MIE = the structural modelling provides direct evidence for the similar binding to the same binding pocket of complex I. (Low) KE1 = measured of complex I activity using substrates of complex I is the most direct measure of KE1 inhibition. (Low) KE2 = measurement of overall oxygen consumption and loss of mitochondrial membrane potential and ATP depletion are direct measurements of mitochondrial functioning. (Low) KE3 = Measurements of the proteasome activity does not completely reflect the complexness that should be captured when addressing this key event. (Medium) KE4= Neurite outgrowth and degeneration are indicative for loss of neuronal cell function. There is uncertainty whether these assays directly reflect the *in vivo* degeneration process of the dopaminergic neurons. Moreover, we have not studied these effects in the presence of supporting glial cells (Medium)

		KE5= not measured. We do not have the appropriate assays available to integrate immune cells (innate and/or adaptive) in the test battery. We cannot exclude that *in vivo* the KE5 is the most critical determinant that should be included in our test methods. Given that this is a rather late KE5 in the AOP, where late KEs have typically a higher degree of uncertainty to be of relevance, we think that lacking the measurements of these KEs will not hamper the overall conclusions.
Similarity of endpoint data (among source compounds)	Low-Medium	Overall, the similarity in the data between rotenone and deguelin is high for all assays. The exception is the neurite outgrowth assay in the normal medium containing glucose. Under these conditions, the potency of rotenone for affecting neurite outgrowth is higher than for deguelin.
Concordance and weight of evidence for justifying the hypothesis	Low	The application of an AOP-based testing strategy using various NAMs allows for an evaluation of read across. The combined data support that rotenone and deguelin have similar behavior in the various test methods but different potency.
Overall	Low	The overall uncertainty for the case study is low. Although there is some uncertainty for a full read across application of the AOP, based on the fact that only one source compound was used in this study. Yet the structure-based modeling has clearly identified the structural determinants that lead to binding complex I, the molecular initiation event of the AOP, providing strong evidence on the molecular domains of deguelin and rotenone that lead to inhibition of complex I.

6.2. Integrated conclusion

In this case study, we evaluated the application of an AOP-based testing strategy and its application for read across. The AOP for inhibition of the mitochondrial complex I of nigrostriatal neurons leads to parkinsonian motor deficits has been assessed using two different rotenoids, the source substance rotenone and the target substance deguelin. For the source compound there is compelling evidence for the induction of Parkinson's-like disorders in experimental models.

We have selected various NAMs that represent the MIE and KEs of the AOP to assess the similarity of deguelin and rotenone. Using structural modelling we determined that deguelin has a similar binding to complex I; both compound share a common pharmacophore that determines the binding to complex I, the MIE of the AOP.

Subsequently, we determined the effect on KE1, inhibition of complex I. Both rotenone and deguelin specifically inhibit complex I activity, without affecting other mitochondrial respiratory complexes. At the level of mitochondrial functioning, KE2, both rotenone and deguelin did decrease the oxygen consumption rate in association with loss of the mitochondrial membrane potential and cellular AOP levels. Rotenone was typically a factor ~3 more potent for the mitochondrial effects than deguelin. Rotenone and deguelin also did slightly affect cellular proteostasis, KE3, albeit at higher concentration than the effect on mitochondrial functioning. Also, here the strongest effects on proteostasis were observed for rotenone. The test methods to evaluate degeneration of dopaminergic neurons, KE4, was based on the neurite outgrowth assays. Here we observed that both rotenone and deguelin did affect the neurite outgrowth, and, depending on the culture condition, the difference in potency between rotenone and deguelin was minimally a factor 3, as also observed for loss of mitochondrial function. Given the consistency of KE1-4, we do not have the appropriate test methods for KE5 in place and therefore cannot overall conclude that all KEs of the AOP:3 are fit for purpose for an AOP-based IATA.

NAM methods to predict the cellular concentrations revealed no differences in the concentrations in the cells and cellular compartments between rotenone and deguelin. The PBPK modelling did predict similar biokinetics of both rotenone and deguelin, with similar distribution of both compounds to the brain.

The combined *in silico* and *in vitro* NAMs indicate that rotenone and deguelin are highly similarly in biological effects, with rotenone being ~3 times more potent than deguelin based on the mitochondrial toxicity effects and the neurite outgrowth assays. Based on the

data deguelin would be expected to cause nigrostriatal neuronal system degeneration *in vivo*. Indeed one recent *in vivo* study has compared the *in vivo* effect of rotenone and deguelin and demonstrated that deguelin can also cause nigrostriatal DA neuron degeneration.

Altogether our current case study demonstrate that an AOP-based testing strategy combining different test methods that cover the various KEs can find application in supporting read across chemical safety assessment.

7. Acknowledgements

The case study was part of the EU ToxRisk project. The core authors of this case study document are Wanda van der Stel[1], Susanne Hougaard Bennekou[2], Giada Carta[3], Julie Eakins[4], Johannes Delp[5], Anna Forsby[6], Hennicke Kamp[7], Ian Gardner[8], Barbara Zdradil[9], Manual Pastor[10], Jose Carlos Gomes[10], Andrew White[11], Thomas Steger-Hartman[12], Erik H.J. Danen[1], Marcel Leist[5], Paul Walker[4], Paul Jennings[3], Bob van de Water[1].

[1]Division of Drug Discovery and Safety, Leiden Academic Centre of Drug Research, Leiden University, Leiden, the Netherlands.

[2]National Food Institute, Technical University of Denmark (DTU), Lyngby, Denmark

[3]Division Molecular and Computational Toxicology, Vrije University Amsterdam, Amsterdam, the Netherlands.

[4]Cyprotex Discovery Ltd., Alderley Park, Macclesfield, Cheshire, United Kingdom.

[5]University of Konstanz, Konstanz, Germany.

[6]Department of Biochemistry and Biophysics, Stockholm University, Stockholm, Sweden.

[7]BASF, Ludwigshafen, Germany.

[8]Certara UK Limited, Sheffield, United Kingdom.

[9]University of Vienna, Austria.

[10]Universitat Pompeu Fabra, Spain.

[11]Unilever, Bedfordshire, United Kingdom.

[12]Bayer, Berlin, Germany.

8. References

Antczak, C. *et al.* (2014). A High-Content Assay Strategy for the Identification and Profiling of ABCG2 Modulators in Live Cells, *Assay and Drug Development Technologies*, Vol. 12, No.1, pp. 2–4. doi: 10.1089/adt.2013.521.

Baba, Y. *et al.* (2015). Deguelin induces apoptosis by targeting both EGFR-Akt and IGF1R-Akt pathways in head and neck squamous cell cancer cell lines. *Biomed Res Int.* 2015:657179.

Barlow B.K., Richfield E.K., Cory-Slechta D.A., and Thirsuchelvam M. 2004. A fetal risk factor for Parkinson's disease. Dev. *Neurosci*. Vol. 4, No. 26, pp. 11-23.

Betarbet, R. *et al.* (2006). Intersecting pathways to neurodegeneration in Parkinson's disease : Effects of the pesticide rotenone on DJ-1, A-synuclein, and the ubiquitin – proteasome system, *Neurobiology of Disease*, Vol. 22, pp. 404–420. doi: 10.1016/j.nbd.2005.12.003.

Betarbet, R. *et al.* (2000). Chronic systemic pesticide exposure reproduces features of Parkinson's disease, *nature neuroscience*, Vol. 26, pp. 1301–1306.

Caboni, P. *et al.* (2004). Rotenone, Deguelin, Their Metabolites, and the Rat Model of Parkinson's Disease, *Chem. Res. Toxicol*., (Figure 1), Vol. 17, No. 11, pp. 1540–1548. doi: 10.1021/tx049867r.

Cheng HC, Burke RE. (2010). The Wld(S) mutation delays anterograde, but not retrograde, axonal degeneration of the dopaminergic nigro-striatal pathway *in vivo*. *J Neurochem*. Vol. 113, No. 3, pp. 683-691. doi:10.1111/j.1471-4159.2010.06632.x

Delp, J. *et al.* (2018). A High-Throughput Approach to Identify Specific Neurotoxicants/Developmental Toxicants in Human Neuronal Cell Function Assays, *Altex*, Vol. 35, No. 2, pp. 235–253. doi: 10.14573/altex.1712182.

De Wilde, R. A. (1986) A case of fatal rotenone poisoning in a child, *J Forensic Sci.,* Vol. 31, No. 4, pp. 1492–1498.

Dhillon, A. S. *et al.* (2008). Pesticide/Environmental Exposures and Parkinson's Disease in East Texas, *Journal of Agromedicine*, Vol. 13, No. 1, pp. 37-48. doi: 10.1080/10599240801986215.

ECHA (2018). Decision on Substance Evaluation (Ziram), European Chemicals Agency, Helsinki, https://echa.europa.eu/documents/10162/1d12a33a-9c6e-e64a-ba40-901b24bdbd0c

EFSA (2017). Scientific Opinion on the investigation into experimental toxicological properties of plant protection products having a potential link to Parkinson's disease and childhood leukaemia. *EFSA Journal,* Vol. 15, Nol. 3, pp. 4691 (325 pp). European Food Safety Authority, Parma. doi:10.2903/j.efsa.2017.4691

Eriksson P. (1996). Developmental neurotoxicology in the neonate-Effects of pesticides and polychlorinated substances. *Arch. Toxicol*. *Suppl*., Vol. 18, pp. 81-88.

Eriksson P., Johansson U., Ahlbom J., and Fredriksson A. (1993). Neonatal exposure to DDT induces increased susceptibility to pyrethroid (bioallethrin) exposure at adult age- Changes in cholinergic muscarinic receptor and behavioral variables. *Toxicology*. Vol. 77, pp. 21-30.

Fendel, U. *et al.* (2008). Biochimica et Biophysica Acta Exploring the inhibitor binding pocket of respiratory complex I, Vol. 1777, pp. 660–665. doi: 10.1016/j.bbabio.2008.04.033.

Greenamyre JT, Sherer TB, Betarbet R, Panov AV. (2001). Complex I and Parkinson's disease. *IUBMB Life.* Vol. 52, No. 3-5, pp. 135-141. doi:10.1080/15216540152845939

Guo, R. *et al.* (2017). Architecture of Human Mitochondrial Respiratory Article Architecture of Human Mitochondrial, *Cell. Elsevier Inc.*, Vol. 170, No. 6, pp. 1247–1249.e12. doi: 10.1016/j.cell.2017.07.050.

Gupta a., Agarwal R., and Shukla G.S. (1993). Functional impairment of the blood-brain barrier following pesticide exposure during early development in rats. *Hum. Exp. Toxicol*. Vol. 18, pp. 174-179.

Higgins, D. S. and Greenamyre, J. T. (1996). Reductase (Complex An Autoradiographic Binding to NADH : Ubiquinone I) of the Electron Transport Chain : Study, *J Neurosci*, Vol. 16, No. 12, pp. 3807–3816.

Holvikari, K. and Kidron, H. (2017). Inhibition of Breast Cancer Resistance Protein and Multidrug Resistance Associated Protein 2 by Natural Compounds and Their Derivatives, *Mol. Pharmaceutics*, Vol. 14, No. 1, pp. 135-146. doi: 10.1021/acs.molpharmaceut.6b00754.

Jain S, Grandits M, Richter L, Ecker GF. (2017). Structure based classification for bile salt export pump (BSEP) inhibitors using comparative structural modeling of human BSEP. *J Comput Aided Mol Des*., Vo. 31, No. 6, pp. 507-521.

Kamel, F. *et al.* (2007). Original Contribution Pesticide Exposure and Self-reported Parkinson's Disease in the Agricultural Health Study, *American Journal of Epidemiology*, Vol. 165, No. 4, pp. 364–374. doi: 10.1093/aje/kwk024.

Krug, A. K. *et al.* (2013). Evaluation of a human neurite growth assay as specific screen for developmental neurotoxicants, *Arch Toxicol*, Vol. 87, No. 12, pp. 2215–2231. doi: 10.1007/s00204-013-1072-y.

Lacher, S. E. *et al.* (2015). P-Glycoprotein Transport of Neurotoxic Pesticides, J Pharmacol Exp Ther., Vol. 335, No. 1, pp. 99–107.

Lu X, Liang Q, Liu W, Zhou L, Li W, Liu H. (2017). Deguelin, an Aurora B Kinase Inhibitor, Exhibits Potent Anti-Tumor Effect in Human Esophageal Squamous Cell Carcinoma. *EBioMedicine,* Vol. 26, pp. 100-111.

Melamed E., Rosenthal J., and Youdim M.B.H. (1990). Immunity of fetal mice to prenatal administration of the dopaminergic neurotoxin 1-methyl-4-phenyl-1,2,3,6-tetrahydropyridine. *J. Neurochem*, Vol. 55, pp. 1427-1431.

Nt, N. G. Á. *et al.* (2005). *In vitro* Search for Synergy Between Flavonoids and Epirubicin on Multidrug-resistant Cancer Cells, In Vivo, Vol. 19, pp. 367–374.

Ntzani, E. E. (2013). Literature review on epidemiological studies linking exposure to pesticides, *EFSA Supporting Publication*, EN-497, 159 pp.

OECD (2018), Adverse Outcome Pathway on Inhibition of the mitochondrial complex I of nigro-striatal neurons leading to parkinsonian motor deficits, Series on Adverse Outcome Pathways No. 7., OECD, Paris. https://doi.org/10.1787/2415170X

Oh SH, Woo JK, Yazici YD, Myers JN, Kim WY, Jin Q, Hong SS, Park HJ, Suh YG, Kim KW, Hong WK, Lee HY. (2007). Structural basis for depletion of heat shock protein 90 client proteins by deguelin. *J Natl Cancer Inst*. Vol. 99, No. 12, pp. 949-61.

Okun, G., Lu, P. and Brandt, U. (1999). Three Classes of Inhibitors Share a Common Binding Domain in Mitochondrial Complex I (NADH : Ubiquinone Oxidoreductase), *J Biol Chem*, Vol. 274, No. 5, pp. 2625–2630.

Ravenstijn, P. G. M. *et al.* (2007). The exploration of rotenone as a toxin for inducing Parkinson's disease in rats, for application in BBB transport and PK–PD experiments, *Journal of Pharmacological and Toxicological Methods*, Vol. 57, pp. 114–130. doi: 10.1016/j.vascn.2007.10.003.

Seo, B. *et al*. (1998). Molecular remedy of complex I defects: Rotenone-insensitive internal NADH-quinone oxidoreductase of Saccharomyces cerevisiae mitochondria restores the NADH oxidase activity of complex I-deficient mammalian cells, *Proc. Natl. Acad. Sci. USA*, Vol. 95, pp. 9167–9171.

Sherer, T. B. *et al.* (2003) Mechanism of Toxicity in Rotenone Models of Parkinson's Disease, *The Journal of Neuroscience*, Vol. 23, No. 34, pp. 10756–10764.

Stiegler, N. V *et al.* (2011). Assessment of Chemical-Induced Impairment of Human Neurite Outgrowth by Multiparametric Live Cell Imaging in High-Density Cultures, *Toxicological Sciences: an Official Journal of the Society of Toxicology*, Vol. 121, No. 1, pp. 73–87. doi: 10.1093/toxsci/kfr034.

Talpade, D. J. *et al.* (2000). *In vivo* Labeling of Mitochondrial Complex I (NADH : Ubiquinone Oxidoreductase) in Rat Brain Using [(3)H] Dihydrorotenone, *J Neurochem*, Vol. 75, No. 6, pp. 2611–2621.

Tanner, C. M. *et al.* (2011). Rotenone, Paraquat, and Parkinson's Disease, *Environmental Health Perspectives*, Vol. 6, pp. 866–872. doi: 10.1289/ehp.1002839.

Terron, A. *et al.* (2019). An adverse outcome pathway for parkinsonian motor deficits associated with mitochondrial complex I inhibition, *Archives of Toxicology*, Vol. 93, 1771 pp, Springer Berlin Heidelberg. doi: 10.1007/s00204-017-2133-4.

Testa, C. M., Sherer, T. B. and Greenamyre, J. T. (2005). Rotenone induces oxidative stress and dopaminergic neuron damage in organotypic substantia nigra cultures, *Molecular Brain Research*, Vol. 134, pp. 109–118. doi: 10.1016/j.molbrainres.2004.11.007.

Thiruchelvam M., Richfield E.K., Goodman B.M., Baggs R.B., and Cory-Slechta D.A. (2002). Developmental exposure to pesticides paraquat and maneb and the Parkinson's disease phenotype. *Neurotox*. Vol. 33, pp. 621-633.

Udeani, G. O. *et al.* (2001). Pharmacokinetics of deguelin , a cancer chemopreventive agent in rats, *Cancer Chemother Pharmacol*, Vol. 47, pp. 263–268. doi: 10.1007/s002800000187.

Wetmore, B. A. *et al.* (2012). Integration of Dosimetry, Exposure, and High-Throughput Screening Data in Chemical Toxicity Assessment, *Toxicol Sci.*, Vol. 125, No. 1, pp. 157–174. doi: 10.1093/toxsci/kfr254.

Log P values in Table 2

- Pubchem = https://pubchem.ncbi.nlm.nih.gov
- Toxnet = https://toxnet.nlm.nih.gov/cgi-bin/sis/search2/r?dbs+hsdb:@term+@rn+@rel+83-79-4
- EBI = https://www.ebi.ac.uk/chembl/compound/inspect/CHEMBL429023; https://www.ebi.ac.uk/chembl/compound/inspect/CHEMBL393417
- Chemspider = http://www.chemspider.com/Chemical-Structure.6500.html?rid=2ac92dcf-5fb4-47ff-8366-1b5c847a81cf; http://www.chemspider.com/Chemical-Structure.97058.html?rid=5ae8e762-d32b-40cb-b5a8-b7303a8b918d
- Chemspider2 = http://www.chemspider.com/Chemical-Structure.97058.html?rid=776d24b8-b5ed-46cd-9833-578925943ce7

Appendix. Data matrix

Chemical ID			
		Target	Source1
CAS		522-17-8	83-79-4
Name		Deguelin	Rotenone
Structure		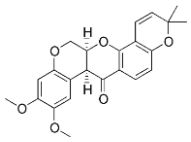	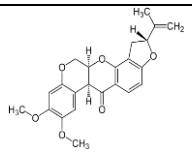
Physical-chemical data			
$logP_{ow}$ (measured value)			
$logP_{ow}$ (calculated value)		3.7-5.03	4.1-4.65
Similarity (Tanimoto Coefficient)			
Similarity 3D (structural modelling complex 1 - AOP MIE)		similar 3D pharmacophore as rotenone for binding complex I.	
Kinetics *In vivo Iin silico*			
Absorption		High/high	High/high
Distribution		High/high	High/high
Metabolism		Moderate/moderate	Moderate/moderate
Excretion		Moderate	Moderate
Supporting data related to the target endpoint(s)			
		Target	Source1
In vivo	Degeneration nigrostriatal dopaminergic neurons		Experimental *in vivo* rat studies repeated dosing
In vitro (BMC_{25} [nM])	KE1: Oxygen consumption neuro intact cells (LUHMES) (IC_{50} nM)	+/- 100	+/- 25
	KE1: Oxygen consumption neuro individual complexes (LUHMES) (IC_{50} nM)	86.1	26.4
	KE1: Oxygen consumption Basal/Max HepG2 (BMC_{25} nM)	537/112	162/50
	KE2: Mitochondrial membrane potential (HepG2_24h) (BMC_{25} nM)	24	3
	KE2: Mitochondrial membrane potential (RPTEC_24h) (BMC_{25} nM)	75	1.7
	KE2: Mitochondrial membrane potential (SH-SY5Y_24h) (BMC_{25} nM)	295	38
	KE2: Lactate production (HepG21_24h) (BMC_{25} nM)	102	75
	KE2: Lactate production (RPTEC/TERT1_24h)(BMC_{25} nM)	191	182
	KE2: Lactate production (SH-SY5Y_24h)(BMC_{25} nM)	5754	120
	KE3: Proteosome assay (LUHMES)	+/- 5000	+/- 5000
	KE3: CHOP-GFP reporter (HepG2) (1st effective conc)	400	80
	KE4: Neurite outgrowth/Viability/ATP (LUHMES) (EC_{50} nM) Glucose	5600/34500/7800	200/36000/40000

	KE4: Neurite outgrowth/Viability/ATP (LUHMES) (EC_{50} nM) Galactose	7.4/152/4.5	2.5/760/4.8
	KE4: Neurite degeneration/Viability (LUHMES) (EC_{50} nM) repeated dose	1000/1585	100/3981
	KE4: Neurite degeneration/Cytotoxicity (SH-SY5Y_24h) (EC_{25} nM)	NA/NA	32/NA
	KE4: Neurite degeneration/Cytotoxicity SH-SY5Y_120h) (EC_{25} nM) repeated dose	10000/10000	12.5/316

Annex 1. Methods

Please refer to the separate publication for the detailed methods in Annex 1: ENV/JM/MONO(2020)33/ANN1

Seahorse

- Complexes
- Whole cells

Mitochondrial Membrane Potential

Mitochondrial viability

- lactate
- resazurin
- ATP levels

Protesome assays

- Proteosome activity
- CHOP-GFP reporters

Neurite outgrowth/degeneration

- glucose
- galactose

Bioavailability

- model
- samples
- mass spectrometry

PBPK

Repeat dosing

Receptor docking